Gas Amplification in a Strong E-Field

This part will be very brief, since my understanding of this subject is very much limited!

Gas Amplification

Average Gas Gain

Twonsend Coefficient

The probability per unit length for a seed electron in a strong E-field producing an additional ionization electron is called the first Townsend coefficient (α). We can write the average increase of electrons (dN) over a path (ds) to be

$$dN = N\,\alpha\,ds$$

The Townsend coefficient is determined by the cross sections for ionizing collisions or excitation collisions leading to secondary ionizations through Penning effect or Jesse effect. These cross sections are a function of the electron's speed or equivalently its energy, which is in turn a function of two scaling variables: "E/(gas density)" and "B/(gas density)", as far as the t- and x-derivatives of the electron state density function on the L.H.S. of Boltzmann eq. can be ignored.

Then the Townsend coefficient, having the dimension of inverse length, must scale with the mean free path inverse and hence should be proportional to the gas density:

$$\alpha = \alpha_0\left(\frac{\boldsymbol{E}}{\rho}, \frac{\boldsymbol{B}}{\rho}\right)\cdot\frac{\rho}{\rho_0}$$

unless E-field variation is so quick that the f(v;x) changes significantly over a few mean free paths.

Taking this condition for granted we can write the average gas gain as a line integral:

$$\bar{G} := \frac{N}{N_0} = \exp\left[\int_A^B ds\,\alpha(E(s))\right]$$

which in general depends on the possible path along which the avalanche develops.

The formula allows one to calculate the average gas gain once the 1st Townsend coefficient is given as a function of the E-field. Strictly speaking, the scaling holds only when we change both the E- and B- fields simultaneously. As far as I know there is no analytic treatment of general E and B configurations. When the E- and B- fields are parallel, however, the longitudinal motion will not be affected by the B-field and hence we can ignore the B-field effect on the Townsend coefficient (recall that the electron energy is characterized by eD/mu which is unaffected).
In the case of uniform E//B, we have

$$\bar{G}(\Delta) = \exp\left[\alpha(V/\Delta)\,\Delta\right]$$

where Δ is the amplification gap and V is the high voltage across it.
This should be a good approximation for a GEM or micromegas in particular. Notice that the Townsend coefficient increases with the E-field. If the E-field is constant, the gas gain increases with the gap. The E-field, however, decreases when the gap is increased. This suggests that the gas gain must attain a maximum for an appropriate gap value, around which the gas gain is stable against gap variation. This is the operation principle of the micromegas.

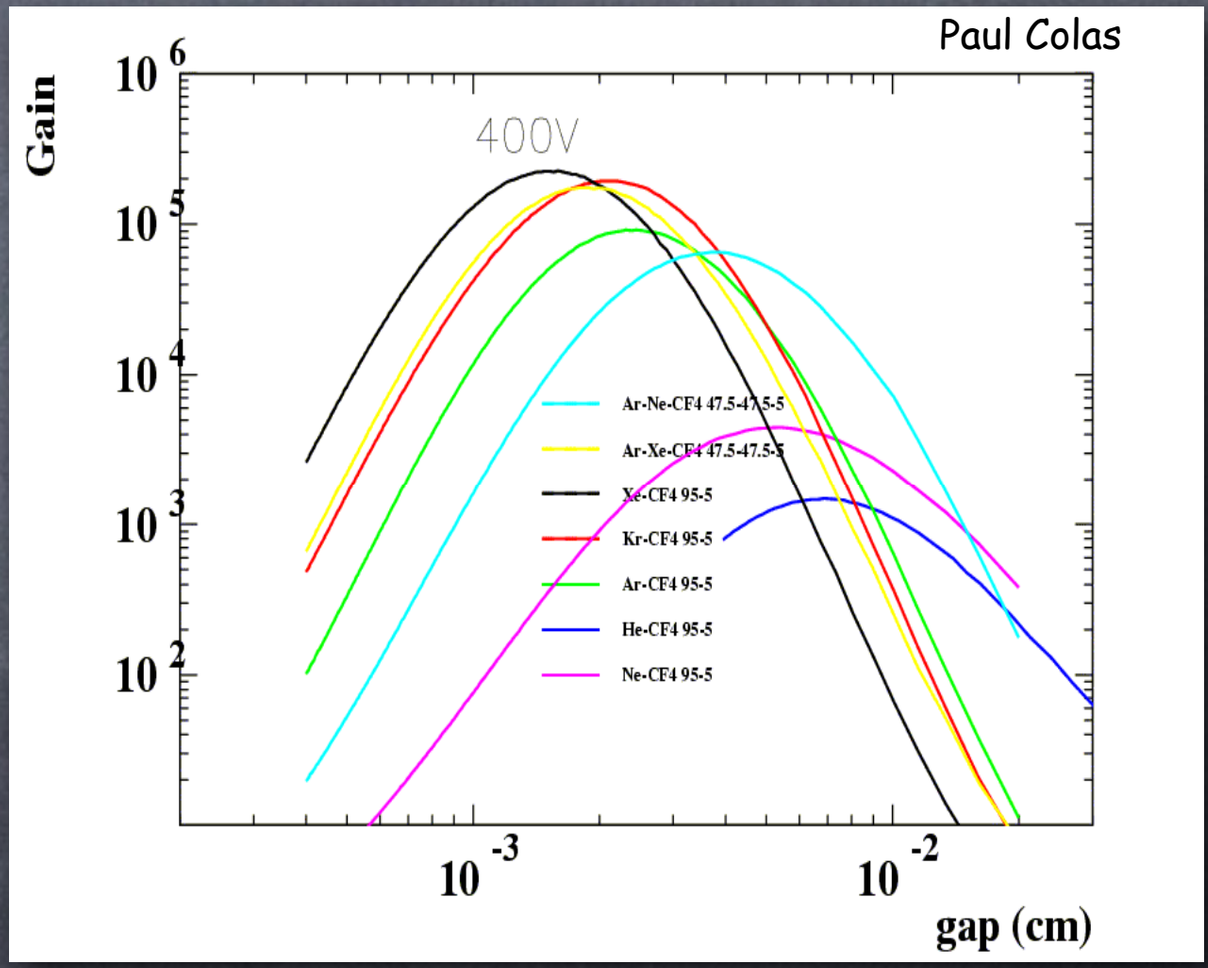

Gas Amplification

Statistics of Avalanche Fluctuation

Alkhazov's Theory (1970)

The avalanche formation involves various mechanisms: impact ionization, Penning and Jesse processes. We consider here the case where the impact ionization dominates.
We further assume a uniform E-field in the amplification region. A B-field, if there is any, should be parallel to the E-field. Now let the probability of getting N electrons at the point x from the beginning of the amplification region be P(N; x), then P(N; x) must satisfy the following self-consistency equation:

$$P(N;x) = \int_0^x dl\, p_{\rm i}(l) \sum_{N'=1}^{N-1} P(N';x-l)P(N-N';x-l)$$

where pi(l) is the probability of 1st ionizing collision taking place at the distance l from the origin of the seed electron.

Graphically we can represent this as in the following figure:

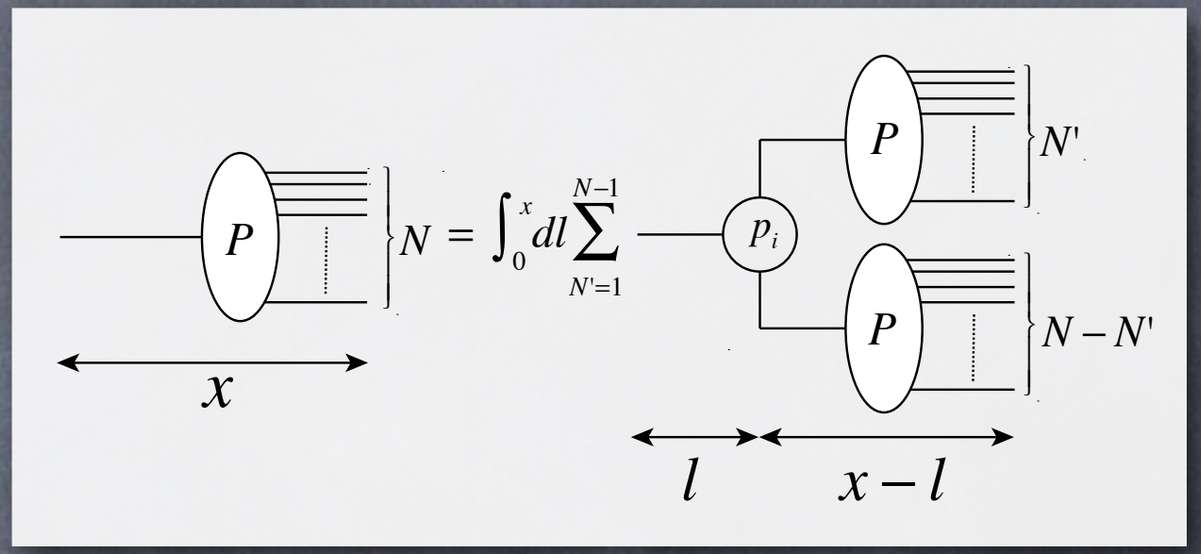

We can define the avalanche fluctuation function as

$$p(z,x) := \bar{N}(x)\, P(\bar{N}(x)z;x)$$

and its n-th moment as

$$\begin{aligned} M_n &:= \int_0^\infty dz\, z^n\, p(z,x) \\ &= \sum_{N=0}^{\infty} \frac{1}{\bar{N}(x)} \left(\frac{N}{\bar{N}(x)}\right)^n \bar{N}(x)\, P(N;x) \end{aligned}$$

Because of the central limit theorem, we expect that the avalanche fluctuation fn. and hence its moments also are determined by the early stage of the avalanche growth, which implies that p(z, x) should become x-independent

$$p(z,x) \to p(z)$$

at large x where

$$\bar{N}(x) \to e^{\alpha x}$$

Keeping these in mind, we can derive from

$$P(N;x) = \int_0^x dl\, p_{\rm i}(l) \sum_{N'=1}^{N-1} P(N';x-l)P(N-N';x-l)$$

an equation for Mn:

$$M_n \;\; = \;\; \sum_{k=0}^{n} \frac{n!}{k!(n-k)!} M_k\, M_{n-k} \int_0^\infty dl\, p_{\rm i}(l)\, e^{-n\,\alpha\, l}$$

This leads us to a recurrence formula:

$$M_n = \sum_{k=1}^{n-1} \frac{n!}{k!(n-k)!} \frac{M_k\, M_{n-k}\, J(n)}{1-2J(n)}$$

with

$$J(n) := \int_0^\infty dl\, p_{\rm i}(l)\, e^{-n\,\alpha\, l}$$

determined by the probability for the 1st ionizing collision.
On the other hand, we have

$$M_0 = M_1 = 1$$

by definition. M1=1 determines the 1st Townsend coefficient:

$$2J(1) = 2\int_0^\infty dl\, p_{\rm i}(l)\, e^{-\alpha\, l} = 1$$

Once pi(l) is given, we can hence calculate Mn recursively.

The self-consistency equation also induces an equation for p(z):

$$p(z) = \frac{1}{\alpha\, z} \int_z^\infty dz' \int_0^{z'} dz''\, p(z'')\, p(z'-z'')\, p_{\rm i}\left(\frac{1}{\alpha} \ln \frac{z'}{z}\right)$$

which can be used to get an approximate solution by iterative substitutions.

The self-consistency equation for p(z)

$$p(z) = \frac{1}{\alpha\, z} \int_z^\infty dz' \int_0^{z'} dz''\, p(z'')\, p(z'-z'')\, p_{\rm i}\left(\frac{1}{\alpha} \ln \frac{z'}{z}\right)$$

implies that the large l behavior of pi(l) controls the behavior of p(z) near z=0. Assuming the exponential shape for the large l limit:

$$p_{\rm i}(l) \to C\, e^{-a\, l} \quad \text{as} \quad l \to \infty$$

where C is a constant, we have

$$p(z) \simeq z^{\frac{a}{\alpha}-1} \int_0^\infty dz' \int_0^{z'} dz''\, p(z'')p(z'-z'')\, \frac{C}{\alpha} z'^{-a/\alpha}$$

near z=0. Denoting

$$\theta := \frac{a}{\alpha} - 1$$

we hence obtain

$$p(z) \simeq C'\, z^\theta$$

where C' is a constant. In the case of Polya distribution, we have

$$\theta = \theta_{\rm pol} := \frac{1}{\sigma^2} - 1$$

Snyder's Model

If the ionization probability is constant as given by the 1st Townsend coefficient:

$$p_{\rm i}(l) = \alpha\, e^{-\alpha\, l}$$

we have an exponential distribution

$$p(z) = e^{-z}$$

as the exact solution to the above equation. This can be easily checked by substituting this in the self-consistency equation. In this case we have

$$M_n = n!$$

We thus have

$$M_2 = 2$$

in particular.
We will see the significance of this number later when we discuss the effective number of seed electrons (Neff). Experimentally we know that M2 is smaller than 2 for GEM and Mircomegas detectors.

Derivations of Recurrence Formulae

$$
\begin{aligned}
M_n &= \int_0^\infty dl\, p_{\rm i}(l) \left(\frac{\bar{N}(x-l)}{\bar{N}(x)}\right)^n \sum_{N=1}^{\infty} \sum_{N'=1}^{N-1} \left(\frac{N' + (N-N')}{\bar{N}(x-l)}\right)^n P(N'; x-l)\, P(N-N'; x-l) \\
&= \int_0^\infty dl\, p_{\rm i}(l) \left(\frac{\bar{N}(x-l)}{\bar{N}(x)}\right)^n \sum_{N=1}^{\infty} \sum_{N'=1}^{N-1} \sum_{k=0}^{n} \frac{n!}{k!(n-k)!} \left(\frac{N'}{\bar{N}(x-l)}\right)^k \left(\frac{N-N'}{\bar{N}(x-l)}\right)^{n-k} \\
&\qquad \times P(N'; x-l)\, P(N-N'; x-l) \\
&= \int_0^\infty dl\, p_{\rm i}(l) \left(\frac{\bar{N}(x-l)}{\bar{N}(x)}\right)^n \sum_{k=0}^{n} \frac{n!}{k!(n-k)!} \sum_{N'=1}^{\infty} \sum_{N-N'=1}^{\infty} \left(\frac{N'}{\bar{N}(x-l)}\right)^k \left(\frac{N-N'}{\bar{N}(x-l)}\right)^{n-k} \\
&\qquad \times P(N'; x-l)\, P(N-N'; x-l) \\
&= \int_0^\infty dl\, p_{\rm i}(l) \left(\frac{\bar{N}(x-l)}{\bar{N}(x)}\right)^n \sum_{k=0}^{n} \frac{n!}{k!(n-k)!} \sum_{N'=1}^{\infty} \left(\frac{N'}{\bar{N}(x-l)}\right)^k P(N'; x-l) \\
&\qquad \times \sum_{N-N'=1}^{\infty} \left(\frac{N-N'}{\bar{N}(x-l)}\right)^{n-k} P(N-N'; x-l) \\
&= \int_0^\infty dl\, p_{\rm i}(l)\, e^{-n\,\alpha\, l} \sum_{k=0}^{n} \frac{n!}{k!(n-k)!} M_k\, M_{n-k}
\end{aligned}
$$

Derivations of Recurrence Formulae

$$
\begin{aligned}
p(z) &= \int_0^\infty dl\, p_{\rm i}(l) \int_0^{ze^{\alpha\, l}} dz''\, e^{\alpha\, l}\, p(z'')\, p(ze^{\alpha\, l} - z'') \\
&= \int_0^\infty dl\, p_{\rm i}(l)\, e^{\alpha\, l} \int_z^\infty dz'\, \delta(z' - ze^{\alpha\, l}) \int_0^{z'} dz''\, p(z'')\, p(z' - z'') \\
&= \int_z^\infty dz' \int_0^{z'} dz''\, p(z'')\, p(z' - z'') \int_0^\infty dl\, p_{\rm i}(l) \delta(z' - ze^{\alpha\, l})\, e^{\alpha\, l} \\
&= \frac{1}{\alpha\, z} \int_z^\infty dz' \int_0^{z'} dz''\, p(z'')\, p(z' - z'')\, p_{\rm i}\left(\frac{1}{\alpha} \ln \frac{z'}{z}\right)
\end{aligned}
$$

Legler's Model

Legler assumed that any ionizing collision may take place only after the seed electron flying over a minimum distance:

$$x_0 := U_0/E$$

so as to gain enough energy for ionization from the E-field. Legler further assumed the probability of ionizing collision being constant after the seed electron having reached the threshold. The probability of the 1st ionizing collision is then given by

$$p_{\rm i}(l) = a_{\rm i}\, e^{-a_{\rm i}(l-x_0)}\theta(l-x_0)$$

As mentioned before, 2J(1) = 1 gives

$$a_{\rm i} = \frac{\alpha}{2e^{-\alpha x_0} - 1} \qquad (0 \le \alpha\, x_0 \le \ln 2)$$

Notice that in the low E-field limit, where

$$\alpha x_0 \to 0 \text{ as } E/\rho \to 0$$

and hence

$$a_{\rm i} \to \alpha \text{ as } E/\rho \to 0$$

converging to Snyder's model.

It is hence important to have a high E-field in the early stage of the avalanche growth in order to suppress gain fluctuation.

From

$$M_n = \sum_{k=1}^{n-1} \frac{n!}{k!(n-k)!} \frac{M_k\, M_{n-k}\, J(n)}{1-2J(n)}$$

with

$$J(n) := \int_0^\infty dl\, p_{\rm i}(l)\, e^{-n\,\alpha\, l}$$

$$M_0 = M_1 = 1$$

we have

$$M_2 = \frac{2\,J(2)}{1-2\,J(2)}$$

which leads us to

$$\sigma^2 = M_2 - 1 = \frac{(2-e^{\alpha\, x_0})^2}{2-(2-e^{\alpha\, x_0})^2}$$

Denoting

$$\kappa := (2-e^{\alpha\, x_0})^2$$

we then obtain

$$\sigma^2 = M_2 - 1 = \frac{\kappa}{2-\kappa} \qquad (0 \le \kappa \le 1)$$

$$\theta = \frac{2(1-\sqrt{\kappa})}{\sqrt{\kappa}} = \frac{\sqrt{\kappa}}{1+\sqrt{\kappa}}\theta_{\rm pol} \le \theta_{\rm pol}$$

The theta parameter controls the behavior near z=0. The inequality

$$\theta = \frac{2(1-\sqrt{\kappa})}{\sqrt{\kappa}} = \frac{\sqrt{\kappa}}{1+\sqrt{\kappa}}\theta_{\rm pol} \leq \theta_{\rm pol}$$

states that the turn over near z=0 is less prominent than that expected from the variance assuming a Polya distribution

$$\theta_{\rm pol} := \frac{1}{\sigma^2} - 1$$

or for the same theta, the variance is smaller than that expected for the Polya.
Legrer's model thus suggests a probability distribution for the gas gain fluctuation, p(z), being non-Polya. Nevertheless, we can calculate the variance by

$$\sigma^2 = M_2 - 1 = \frac{(2-e^{\alpha\, x_0})^2}{2-(2-e^{\alpha\, x_0})^2}$$

with

$$x_0 := U_0/E$$

If we set

$$U_0 = U_I \,:\, \text{ionization pot.}$$

and define

$$\chi := \frac{\alpha\, U_I}{E}$$

we have

$$\sigma^2 = M_2 - 1 = \frac{(2-e^{\chi})^2}{2-(2-e^{\chi})^2}$$

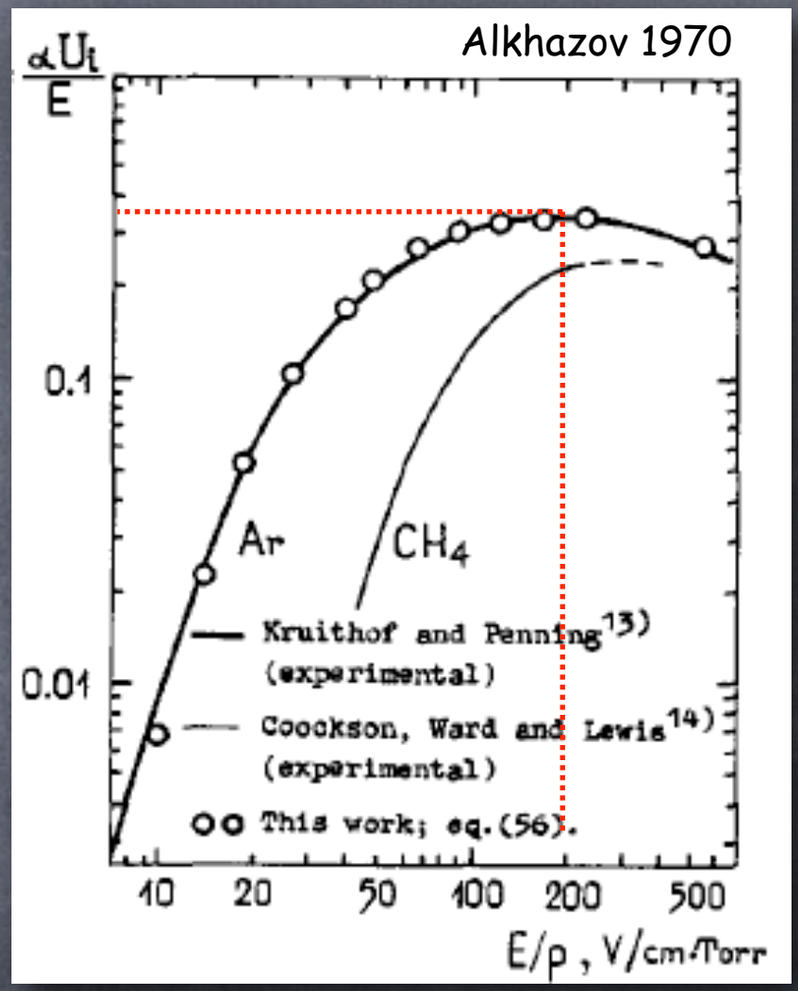

The variance depends on the E-field. The data suggest

$$\sigma^2 = M_2 - 1 \gtrsim 0.2$$

for Ar.

Sample Calculations

Monte Carlo generated gain fluctuation distributions with Legler's model are shown below for chi = 0.1, 0.2, and 0.3:

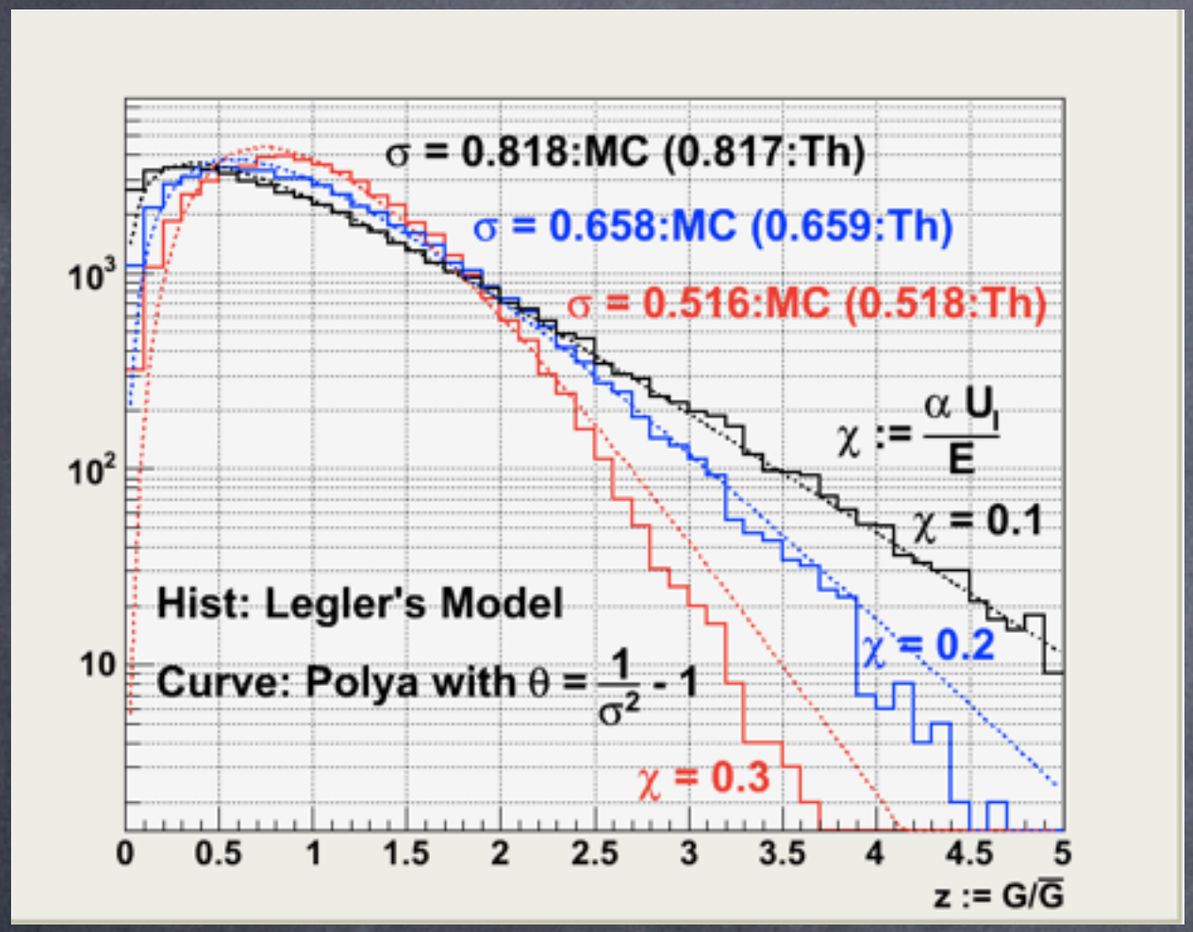

As predicted, Legler's model gives less prominent turnover near z=0 and a shorter tail in the high z region than the Polya distribution with the same sigma value.

Alkhazov's theory predicts

$$\sigma^2 = \frac{(2 - e^{\chi})^2}{2 - (2 - e^{\chi})^2}$$

with

$$\chi := \frac{\alpha U_I}{E}$$

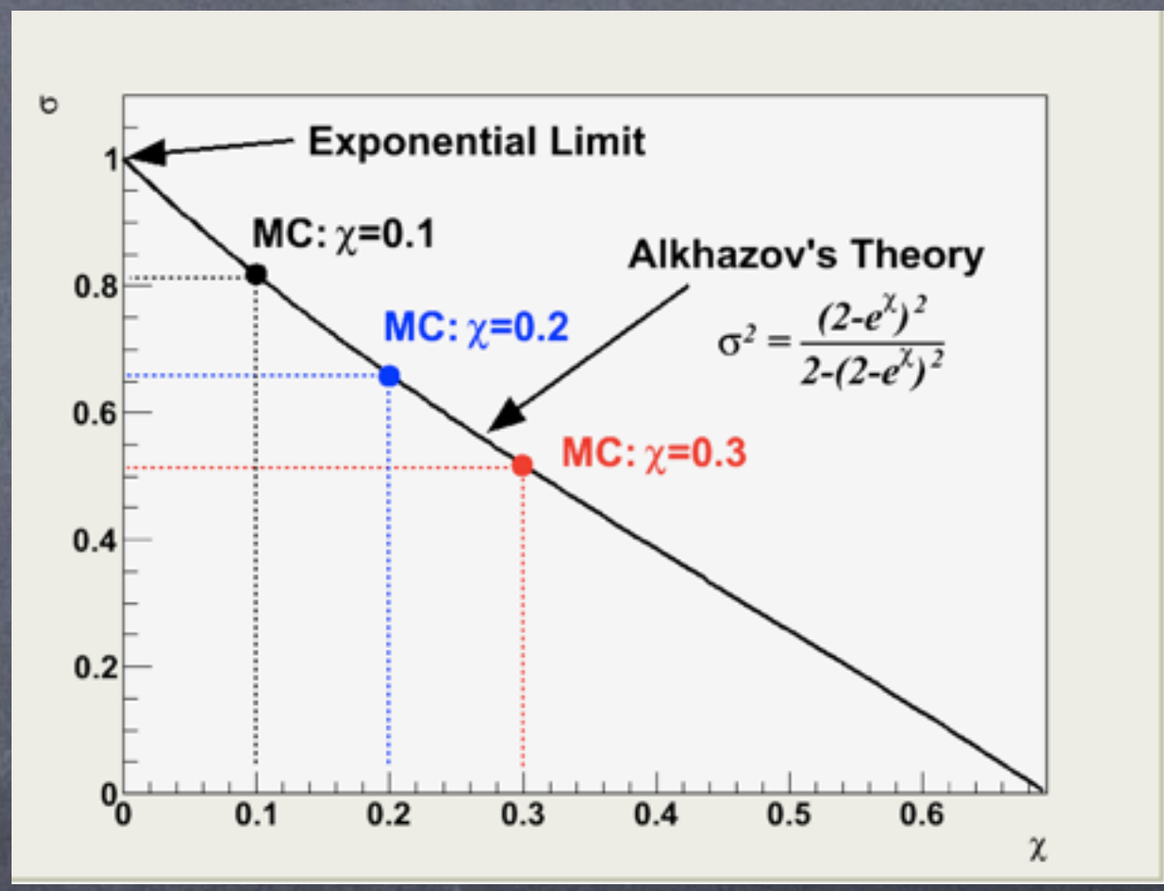

As indicated in the figure, the predictions by Alkhazov's theory agree very well with the Monte Carlo results.

Excursus on Legler's Model

Assuming that the electron accelerates uniformly from at rest until the 1st ionization collision, we have the probability of encountering the 1st ionization collision at distance, l=l, given by

$$p_i(l)dl = P\left(0, \int_0^l dl' n\sigma((V/\Delta)l')\right) \cdot P\left(1, \int_l^{l+dl} dl' n\sigma((V/\Delta)l')\right)$$

where P(m,mu) is the Poisson probability

$$P(m,\mu) = \frac{\mu^m}{m!} e^{-\mu}$$

Substituting the following assumption by Legler for the cross section:

$$\sigma(\epsilon) = \sigma_0\,\theta(\epsilon - U_0)$$

we obtain

$$\int_0^l dl' n\sigma((V/\Delta)l') = n\sigma_0(l - x_0)\theta(l - x_0)$$

$$\int_l^{l+dl} dl' n\sigma((V/\Delta)l') = n\sigma_0\theta(l - x_0)\,dl$$

with $x_0 := (U_0/V)\Delta$

and, hence,

$$p_i(l) = e^{-n\sigma_0(l-x_0)} n\sigma_0\theta(l - x_0)$$

which implies

$$a_i = n\sigma_0$$

sigma0 is a kind of effective cross section and in general depends on the distribution of the electron energy or equivalently (E/n).

Townsend coefficient is given by

$$a_\mathrm{i} = \frac{\alpha}{2e^{-\alpha x_0} - 1} \qquad (0 \le \alpha\, x_0 \le \ln 2)$$

with $x_0 := (U_0/V)\Delta$

Introducing scaling variables eta and chi:

$$\eta := a_i x_0 = n\sigma_0 x_0$$

$$\chi := \alpha x_0$$

and rewriting this, we get

$$\eta = \frac{\chi}{2e^{-\chi} - 1}$$

On the other hand the full gain is given by

$$\ln G = \alpha\Delta = \chi\delta$$

with $\delta := \Delta/x_0 = V/U_0$

Differentiating both sides by some variable X, we get, in general,

$$\frac{dG}{G} = \left[\left(\frac{\partial\chi}{\partial\eta}\right)\left(\frac{\partial\eta}{\partial X}\right)\delta + \chi\left(\frac{\partial\delta}{\partial X}\right)\right] X\left(\frac{dX}{X}\right)$$

Differentiating the logarithms of the both sides of the defining eq. of eta on the previous page, we have, on the other hand,

$$\begin{aligned} 1/\eta &= \left[\frac{1}{\chi} + \frac{\eta}{\chi} 2e^{-\chi}\right]\left(\frac{\partial\chi}{\partial\eta}\right) \\ &= \left[\frac{1}{\chi} + \frac{\eta}{\chi}\left(\frac{\chi}{\eta}+1\right)\right]\left(\frac{\partial\chi}{\partial\eta}\right) \\ &= \frac{1}{\chi}(1+\chi+\eta)\left(\frac{\partial\chi}{\partial\eta}\right) \end{aligned}$$

which leads us to

$$\left(\frac{\partial\chi}{\partial\eta}\right) = \frac{\chi}{\eta(1+\chi+\eta)}$$

Putting them together, we arrive at

$$\frac{dG}{G} = \left[\left(\frac{\chi}{1+\chi+\eta}\right)\frac{1}{\eta}\left(\frac{\partial\eta}{\partial X}\right)\delta + \chi\left(\frac{\partial\delta}{\partial X}\right)\right] X\left(\frac{dX}{X}\right)$$

with

$$\eta = \sigma_0\left[\frac{V/\Delta}{n}\right] U_0 \left(\frac{V/\Delta}{n}\right)^{-1}$$

$$\delta = V/U_0$$

$$\chi = \frac{\ln G}{\delta} \quad \text{and} \quad \eta = \frac{\chi}{2e^{-\chi}-1}$$

Case [1] X=Delta

For instance, we have, for X=Delta,

$$\frac{1}{\eta}\left(\frac{\partial\eta}{\partial\Delta}\right) = \frac{1}{\sigma_0}\left(\frac{\partial\sigma_0}{\partial\varepsilon}\right)\left(\frac{\partial\varepsilon}{\partial\Delta}\right) + \frac{1}{\Delta} \quad \text{and} \quad \frac{\partial\delta}{\partial\Delta} = 0$$

where we have introduced a scaling variable:

$$\varepsilon := \frac{E}{n} = \frac{V/\Delta}{n} \quad \text{, leading to} \quad \frac{\partial\varepsilon}{\partial\Delta} = -\varepsilon\frac{1}{\Delta}$$

Putting them together, we arrive at

$$\frac{dG}{G} = \left(\frac{\chi}{1+\chi+\eta}\right)\left[1 - \frac{\varepsilon}{\sigma_0}\left(\frac{\partial\sigma_0}{\partial\varepsilon}\right)\right]\delta\left(\frac{d\Delta}{\Delta}\right)$$

As shown at the beginning of this chapter, we can make the coefficient vanish by tuning Delta and V depending on the gas parameters such as n, sigma0, and U0.

Stability condition reads

$$\frac{\partial \sigma_0}{\partial \varepsilon} = \frac{\sigma_0}{\varepsilon}$$

Case [2] X=n

Similarly, we have, for X=n,

$$\frac{1}{\eta}\left(\frac{\partial \eta}{\partial n}\right) = \left[1 - \frac{\varepsilon}{\sigma_0}\left(\frac{\partial \sigma_0}{\partial \varepsilon}\right)\right]\left(\frac{1}{n}\right) \quad \text{and} \quad \frac{\partial \delta}{\partial n} = 0$$

and, hence,

$$\frac{dG}{G} = \left(\frac{\chi}{1+\chi+\eta}\right)\left[1 - \frac{\varepsilon}{\sigma_0}\left(\frac{\partial \sigma_0}{\partial \varepsilon}\right)\right]\delta\left(\frac{dn}{n}\right)$$

Notice that the coefficient is the same as in the case of X=Delta, implying that the gain is stabilized against the gas density change if it has been stabilized against the change in the gap, Delta. This is probably another advantage of micromegas.

Case [3] X=V

In this case, we have

$$\frac{1}{\eta}\left(\frac{\partial \eta}{\partial V}\right) = \left[1 + \frac{\varepsilon}{\sigma_0}\left(\frac{\partial \sigma_0}{\partial \varepsilon}\right)\right]\left(\frac{1}{V}\right) \quad \text{and} \quad \frac{\partial \delta}{\partial V} = \delta\frac{1}{V}$$

and, hence,

$$\frac{dG}{G} = \left[\left(\frac{1}{1+\chi+\eta}\right)\left\{1 + \frac{\varepsilon}{\sigma_0}\left(\frac{\partial \sigma_0}{\partial \varepsilon}\right)\right\} + 1\right]\chi\delta\left(\frac{dV}{V}\right)$$

If the coefficient has been tuned to make the Delta- and n-dependences vanish to the 1st order as in the case of micromegas, we have

$$\frac{dG}{G} = \left[\left(\frac{2}{1+\chi+\eta}\right) + 1\right]\chi\delta\left(\frac{dV}{V}\right)$$

Note:

$$\eta = \sigma_0\left[\frac{V/\Delta}{n}\right]U_0\left(\frac{V/\Delta}{n}\right)^{-1}$$

with $\varepsilon := \frac{E}{n} = \frac{V/\Delta}{n}$

$$\chi = \frac{\ln G}{\delta} \qquad \delta = V/U_0$$

$$\eta = \frac{\chi}{2e^{-\chi} - 1}$$

From the chi data given as a function of E/n, we can estimate eta(E/n), which in turn gives sigma_0[E/n]. We can then calculate numerically the derivative of sigma_0 with respect to E/n.

Extension to a nonuniform E field

Consider first the avalanche development in a uniform E field. Dividing the amplification region (0,x) into two parts (0,l), (l,x).

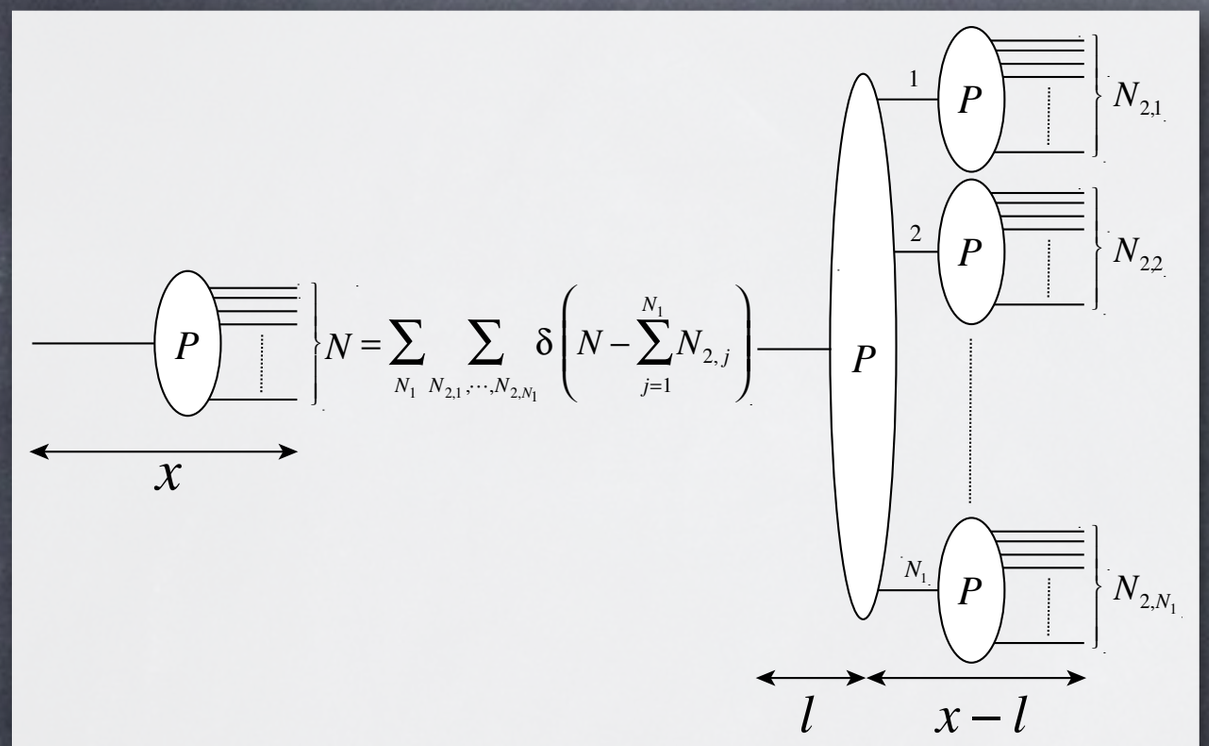

The self-consistency equation for this division reads

$$P(N;x) = \sum_{N_1} \sum_{N_{2,1},\cdots,N_{2,N_1}} \delta\left(N - \sum_{j=1}^{N_1} N_{2,j}\right) \times P(N_1;l) \left(\prod_{j=1}^{N_1} P(N_{2,j};x-l)\right)$$

Here we have assumed that N1 2nd stage avalanches develop independently. The average of N is then given by

$$\begin{aligned} \bar{N}_{12} &= \sum_{N_{12}} P(N_{12};x)\, N_{12} \\ &= \sum_{N_1} \sum_{N_{2,1},\cdots,N_{2,N_1}} N_1\, N_{2,j} P(N_1;l) \left(\prod_{j=1}^{N_1} P(N_{2,j};x-l)\right) \\ &= \bar{N}_1\, \bar{N}_2 \end{aligned}$$

which leads us to a functional equation

$$\bar{N}(x) = \bar{N}(l)\, \bar{N}(x-l)$$

Noting that Nbar(0)=1, we have from this

$$\begin{aligned} \frac{d\bar{N}}{dx}(x) &= \lim_{l\to 0} \frac{\bar{N}(x) - \bar{N}(x-l)}{l} \\ &= \lim_{l\to 0} \bar{N}(x-l)\, \frac{\bar{N}(l) - \bar{N}(0)}{l} \\ &= \bar{N}(x)\, \left.\frac{d\bar{N}}{dx}\right|_{x=0} \end{aligned}$$

We find again the familiar equation

$$\frac{d\bar{N}}{dx} = \alpha\, \bar{N} \quad \text{with} \quad \alpha := \left.\frac{d\bar{N}}{dx}\right|_{x=0}$$

where α is the 1st Townsend coefficient.

This eq. allows us to extend our uniform E-field result to a nonuniform case

$$\bar{G}(x) := \bar{N}(x) = \exp\left[\int_0^x dl\,\alpha(l)\right]$$

This is none other than the average gas gain formula we have derived before.

Let us now consider the variance of the avalanche fluctuations:

$$\overline{(N_{12})^2} - \left(\bar{N}_{12}\right)^2 := \sum P(N_{12};x)\,(N_{12})^2 - \left(\bar{N}_{12}\right)^2$$

$N_1 2$

Recalling the self-consistency equation

$$P(N;x) = \sum_{N_1} \sum_{N_{2,1},\cdots,N_{2,N_1}} \delta\left(N - \sum_{j=1}^{N_1} N_{2,j}\right) \times P(N_1;l)\left(\prod_{j=1}^{N_1} P(N_{2,j};x-l)\right)$$

we have

$$\overline{(N_{12})^2} = \sum_{N_1} \sum_{N_{2,1},\cdots,N_{2,N_1}} P(N_1;l)\left(\prod_{j=1}^{N_1} P(N_{2,j};x-l)\right)\left(\sum_{j=1}^{N_1} N_{2,j}\right)^2$$

which leads us to

$$\begin{aligned}\overline{(N_{12})^2} &= \sum_{N_1} P(N_1;l)\left[N_1\,\overline{(N_2)^2} + \left((N_1)^2 - N_1\right)(\bar{N}_2)^2\right] \\ &= \bar{N}_1\left(\overline{(N_2)^2} - (\bar{N}_2)^2\right) + \overline{(N_1)^2}(\bar{N}_2)^2\end{aligned}$$

Denoting

$$\overline{N^2} - \bar{N}^2 := \bar{N}^2\, f(\bar{N})$$

we arrive at

$$f(\bar{N}_1\,\bar{N}_2) = f(\bar{N}_1) + (\bar{N}_1)^{-1} f(\bar{N}_2)$$

or

$$f(\bar{N}(x)) = f(\bar{N}(l)) + (\bar{N}(l))^{-1} f(\bar{N}(x-l))$$

If the gain of the 1st stage is large, the fluctuation in the 2nd stage is negligible, being consistent with naive expectation. Differentiating both sides with respect to x and then taking l-to-x limit, we get

$$\frac{df}{d\bar{N}}\frac{d\bar{N}}{dx} = \frac{1}{\bar{N}}\left(\frac{df}{d\bar{N}}\right)_{x=0}\left(\frac{d\bar{N}}{dx}\right)_{x=0}$$

Recalling that

$$\frac{d\bar{N}}{dx} = \alpha\bar{N} \quad \text{and} \quad \bar{N}(0) = 1$$

we obtain

$$\frac{df}{d\bar{N}} = \frac{1}{\bar{N}^2}\left(\frac{df}{d\bar{N}}\right)_{x=0} =: \frac{C}{\bar{N}^2}$$

General solution to this equation is

$$f(\bar{N}) = C' - \frac{C}{\bar{N}}$$

We need to impose the boundary condition

$$f(\bar{N}(0)) = f(1) = 0$$

since

$$P(N;0) = \delta(N-1)$$

which requires

$$C' = C$$

Denoting

$$f_0 := f(\infty) = C$$

we can rewrite the equation for f in the following form:

$$\frac{df}{d\bar{N}} = \frac{f_0}{\bar{N}^2}$$

This equation allows us to extend our uniform field results to a nonuniform field.

Recalling

$$\bar{G}(x) := \bar{N}(x) = \exp\left[\int_0^x dl\,\alpha(l)\right]$$

we arrive at

$$f\left(\bar{G}(x)\right) = \int_0^x dx'\,\alpha(x')\frac{f_0(x')}{[\bar{G}(x')]^2}$$

From this and

$$f \equiv \sigma^2 =: \frac{1}{\theta_{\mathrm{pol}}+1}$$

we can calculate the Polya parameter if the Townsend coefficient and f0 are known. Notice that the avalanche fluctuation is in general non-Polya. Nevertheless we may use the Polya parameter as an index.

In the case of Legler's model, we have

$$f_0(x) = \frac{(2-e^{\chi(x)})^2}{2-(2-e^{\chi(x)})^2}$$

with

$$\chi(x) := \alpha(x)\,x_0(x) = \frac{\alpha(x)\,U_0}{E(x)}$$

Central Limit Theorem

Sketch of Its Proof

Characteristic Function

The characteristic function of a probability distribution function P(x) is defined by

$$\phi(s) := \int dx\, e^{isx}\, P(x)$$

which is essentially the Fourier transform of the p.d.f. and hence uniquely specifies it. The characteristic function comes in handy for calculations of moments:

$$M_n := \int dx\, x^n\, P(x)$$

By definition, we have

$$\begin{aligned} M_0 &= 1 \\ M_1 &= \bar{x} \\ M_2 &= \sigma^2 + \bar{x}^2 \end{aligned}$$

Once a characteristic function is given, we can calculate these moments as

$$M_n = (-i)^n \left.\frac{d^n}{ds^n}\phi(s)\right|_{s=0}$$

Examples

For instance, the characteristic function of a Gaussian distribution is

$$\begin{aligned} \phi_G(s) &= \int_{-\infty}^{+\infty} dx\, e^{isx} \frac{1}{\sqrt{2\pi}\sigma} e^{-\frac{(x-\bar{x})^2}{2\sigma^2}} \\ &= e^{-\frac{1}{2}\sigma^2 s^2 + i\bar{x}s} \end{aligned}$$

It is easy to make sure that the first three moments obtained from this characteristic function indeed coincide the above.

$$\begin{aligned} M_1 &= \bar{x} \\ M_2 &= \sigma^2 + \bar{x}^2 \end{aligned}$$

For an exponential distribution, we have

$$\begin{aligned}\phi_E(s) &= \int_0^{+\infty} dx\, e^{isx} \frac{1}{\lambda} e^{-x/\lambda} \\ &= (1 - is\lambda)^{-1}\end{aligned}$$

and hence

$$\begin{aligned}M_1 &= \bar{x} = \lambda \\ M_2 &= \sigma^2 + \bar{x}^2 = 2\lambda^2\end{aligned}$$

For a Polya distribution

$$P_P(x) = \frac{(\theta+1)^{\theta+1}}{\Gamma(\theta+1)} x^\theta e^{-(\theta+1)x}$$

we have

$$\begin{aligned}\phi_P(s) &= \int_0^{\infty} dx\, e^{isx} \frac{(\theta+1)^{\theta+1}}{\Gamma(\theta+1)} x^\theta e^{-(\theta+1)x} \\ &= \left(\frac{\theta+1}{\theta+1-is}\right)^{\theta+1}\end{aligned}$$

The 1st and the 2nd moments obtained from the characteristic function are

$$\begin{aligned}M_1 &= \bar{x} = 1 \\ M_2 &= \sigma^2 + \bar{x}^2 = \frac{2+\theta}{1+\theta}\end{aligned}$$

from which we have

$$\begin{aligned}\bar{x} &= 1 \\ \sigma^2 &= \frac{1}{1+\theta}\end{aligned}$$

If theta=0, the Polya distribution becomes an exponential one with lambda=1 as is clearly seen either from the definition or from its characteristic function.

The Polya distribution becomes a delta-function in the limit of theta going to infinity as is easily seen from its characteristic function:

$$\begin{aligned}\phi_P(s) &= \left(\frac{\theta+1}{\theta+1-is}\right)^{\theta+1} \\ &\to e^{is} \quad \text{as } \theta \to \infty\end{aligned}$$

The asymptotic form coincides with the characteristic function for a Gaussian with a mean value of unity and with a zero width.

Composition Rules

A p.d.f. for a random variable x induces a p.d.f. for a variable (ax). The characteristic function for (ax) is then given by

$$\phi_{ax}(s) = \int d(ax)\, e^{is(ax)}\, \frac{1}{a} P(x) = \phi_x(as)$$

The characteristic function for (x+a) is

$$\phi_{x+a} = \int d(x+a)\, e^{is(x+a)}\, P(x) = e^{ias}\, \phi_x(s)$$

A p.d.f. for a variable x1 and another p.d.f. for a variable x2 induce a p.d.f. for their sum (x1+x2). The characteristic function for this reads

$$\begin{aligned} \phi_{1+2}(s) &= \int dx\, e^{isx} \int dx_1 \int dx_2\, P_1(x_1)\, P_2(x_2) \\ &\qquad \times \delta\left(x - (x_1 + x_2)\right) \\ &= \phi_1(s) \cdot \phi_2(s) \end{aligned}$$

For N variables with the same p.d.f., we get

$$\phi_N(s) = [\phi(s)]^N$$

Proof of Central Limit Theorem

For a given a set of N variables x1, ..., xN, obeying the same p.d.f.: P(x), we consider the distribution of

$$z := \frac{1}{\sqrt{N}\sigma} \sum_{i=1}^{N} (x_i - \bar{x})$$

The characteristic function for this is

$$\phi_z(s) = [\phi_{x-\bar{x}}(s/\sqrt{N}\sigma)]^N$$

Recall now that we can expand phi in terms of moments as follows

$$\begin{aligned} \phi_{x-\bar{x}}(s/\sqrt{N}\sigma) &= \sum_{k=0}^{\infty} \frac{(is/\sqrt{N}\sigma)^k}{k!} M_k \\ &= 1 - \frac{s^2}{2N} + O\left(\frac{1}{N^{3/2}}\right) \end{aligned}$$

In the large N limit, we hence have

$$\begin{aligned} \phi_z(s) &= [\phi_{x-\bar{x}}(s/\sqrt{N}\sigma)]^N \\ &\to \lim_{N\to\infty} \left[1 - \frac{s^2}{2N}\right]^N = e^{-\frac{1}{2}s^2} \end{aligned}$$

implying that the p.d.f. for z is a Gaussian centered at zero with a variance of 1.

Creation of Signals

This part will also be very brief, though practically and technically very important.

Signals on Electrodes

In the Case of Conductive Electrodes

Statement of the Problem

As we have seen, primary and 2ndary track electrons drift towards a gas amplification region experiencing diffusion (and some-times absorption and recombination, too). They act as seeds to individual avalanches. Depending on the gas amplification device in use, the avalanche locations, shapes, and sizes will be different. Nevertheless, as long as the space charge effect is negligible the electrons and the ions in each avalanche drift along the paths determined by the E- and B-field experiencing further diffusion until eventually collected by electrodes that terminate the paths. If the electrodes are made of conductive materials, the E-field adjusts itself instantaneously to the movement of the electrons and the ions.

We can hence treat the problem of solving for the charge induced on each electrode electro-statically, assuming that at every instance the avalanche charges are fixed at definite points in space. The signal time development is then entirely determined by the locations of avalanche charges as a function of time. Since the net charge on the electrode in question is the sum of contributions from individual charges, it suffices to consider a single charge "qi" fixed at some point "xi" in the anode-cathode gap. What we need is the signal charge "Qa" on a-th electrode as a function of "xi":

$$Q_a(\boldsymbol{x_i}) = q_i \, F_a(\boldsymbol{x}_i)$$

from which we can calculate the net signal:

$$Q_a(t) = \sum_i q_i \, F_a(\boldsymbol{x}_i(t))$$

To solve the problem of finding out the response function Fa(x), a theorem known as the reciprocal theorem comes in handy. Let us hence discuss it here.

We consider here a set of localized charge distributions in a dielectric medium, a gas in our case, each of which, say i-th charge distribution rho_i, must satisfy Maxwell's equation

$$\nabla \cdot (\epsilon \nabla \phi_i) = -4\pi \rho_i,$$

with

$$\boldsymbol{D} = \epsilon \boldsymbol{E}$$

where phi_i is the corresponding electrostatic potential, and the condition

$$\phi_i(\boldsymbol{x}) = \text{const.} = V_{i,a} \quad \text{for} \quad \boldsymbol{x} \in D_a$$

must be satisfied, if there are n conductors (D_a; a = 1,..,n). Such phi_i and rho_i are then physically realizable and comprise possible solutions of the Maxwell equation for electrostatic fields.

We are interested in the relation between different solutions, say i-th and j-th. This connection is known as the reciprocal theorem which we now prove below.

Reciprocal Theorem

If (phi_i, rho_i) and (phi_j, rho_j) are solutions of the Maxwell equation for electrostatic fields, they are related by

$$\int d^3\boldsymbol{x}\, \rho_i \phi_j = \int d^3\boldsymbol{x}\, \rho_j \phi_i$$

Proof:

By integrating by parts, the L.H.S. can be transformed into the R.H.S. as follows:

$$\begin{aligned}
L.H.S. &= \int d^3\boldsymbol{x} \left(\frac{1}{4\pi} \nabla \cdot (-\epsilon \nabla \phi_i) \right) \phi_j \\
&= -\frac{1}{4\pi} \int d^3\boldsymbol{x}\, \nabla \cdot (\epsilon \phi_j \nabla \phi_i) + \frac{1}{4\pi} \int d^3\boldsymbol{x}\, \epsilon \nabla \phi_j \cdot \nabla \phi_i \\
&= \frac{1}{4\pi} \int d^3\boldsymbol{x}\, \epsilon \nabla \phi_j \cdot \nabla \phi_i \\
&= \frac{1}{4\pi} \int d^3\boldsymbol{x}\, \nabla \cdot (\phi_i \epsilon \nabla \phi_j) - \frac{1}{4\pi} \int d^3\boldsymbol{x}\, \nabla \cdot (\epsilon \nabla \phi_j) \phi_i \\
&= \int d^3\boldsymbol{x} \left(\frac{1}{4\pi} \nabla \cdot (-\epsilon \nabla \phi_j) \right) \phi_i \;=\; R.H.S.
\end{aligned}$$

QED

If the proof looks too mathematical to you, just note that the charge distribution can be written in the form:

$$\rho_i(\boldsymbol{x}) = \sum_a e_{i,a}\,\delta^3(\boldsymbol{x} - \boldsymbol{x}_{i,a})$$

and the corresponding solution should be

$$\phi_i(\boldsymbol{x}) = \sum_a \frac{e_{i,a}}{|\boldsymbol{x} - \boldsymbol{x}_{i,a}|}$$

then the reciprocal theorem just becomes a trivial identity:

$$\sum_a e_{i,a} \sum_b \frac{e_{j,b}}{|\boldsymbol{x}_{i,a} - \boldsymbol{x}_{j,b}|} = \sum_b e_{j,b} \sum_a \frac{e_{i,a}}{|\boldsymbol{x}_{j,b} - \boldsymbol{x}_{i,a}|}$$

Now we divide the charge distribution into two parts, charges on the electrodes and the charges in the space between the anode and the cathode:

$$\rho_i(\boldsymbol{x}) = \sum_a \rho_{i,a}(\boldsymbol{x}) + \tilde{\rho}(\boldsymbol{x})$$

Since the potential has the same value at any point on a single conductor, we have

$$\int d^3\boldsymbol{x} \sum_a \rho_{i,a}\phi_j =: \sum_a V_{j,a} \int d^3\boldsymbol{x}\,\rho_{i,a} =: \sum_a V_{j,a} Q_{i,a}$$

where $V_{j,a}$ is the potential of a-th electrode for solution j and $Q_{i,a}$ is the total charge on it for solution i.

The reciprocal theorem then reads

$$\sum_a Q_{i,a}V_{j,a} + \int d^3\boldsymbol{x}\,\tilde{\rho}_i\phi_j = \sum_a Q_{j,a}V_{i,a} + \int d^3\boldsymbol{x}\tilde{\rho}_j\phi_i$$

Procedure to Find Solutions

The above form of the reciprocal theorem will prove very useful as we will see below. If there is no avalanche charge

$$\tilde{\rho} = 0$$

we have

$$\sum_a V_{i,a}Q_a = \sum_a Q_{i,a}V_a$$

where I have omitted suffix "j" assuming it represents a new solution for a new voltage configuration {Va} other than "i"s. If we have as many independent solutions as the number of conductors "n", this matrix eq. uniquely specifies the vector {Qa}.

We can write this as

$$[Q_a] = [V_{i,a}]^{-1}[Q_{i,b}][V_b] =: [C_{ab}][V_b]$$

where [Cab] is a generalization of capacity and is symmetric and independent of the choice of the n solutions. It is completely determined by the nature of the dielectric medium and the geometry of the electrodes as we see below.

Notice first that the above eq. must hold also for "j" belonging to "i"s. We hence have

$$[Q_{j,a}]^T = [V_{i,a}]^{-1}[Q_{i,b}][V_{j,b}]^T = [C_{ab}][V_{j,b}]^T$$

Noting that a, b, i, and j are dummy, we get

$$[C_{ab}]^T = [V_{j,b}]^{-1}[Q_{j,a}] = [C_{ab}]$$

which means [Cab] is symmetric. Let us now prove that [Cab] does not depend on the choice of solutions. Assume that we have another set of "n" independent solutions

$$(V'_{i,a}, Q'_{i,a}) \quad (i = 1, \cdots, n)$$

which can be expanded as

$$[V'_{i,a}] = [A_{ij}][V_{j,a}]$$

and

$$[Q'_{i,a}] = [A_{ik}][Q_{k,a}]$$

The [C'ab] defined with the new set of solutions is then given by

$$\begin{aligned} [C'_{ab}] &= [V'_{i,a}]^{-1}[Q'_{i,b}] \\ &= [V_{i,a}]^{-1}[A_{ij}]^{-1}[A_{ik}][Q_{k,b}] \\ &= [V_{i,a}]^{-1}[Q_{k,b}] \;=\; [C_{ab}] \end{aligned}$$

QED

Now let us move on to the problem with an avalanche charge distribution in the space between the electrodes. The solution to the Maxwell eq. can be written as the sum

$$\phi = \phi_0 + \tilde{\phi}$$

where ϕ_0 is the solution without the space charge under a given voltage configuration {Va} and $\tilde{\phi}$ is the solution with the space charge and with all the electrodes grounded so as not to change the voltages given to the individual electrodes.

Signal charge can then be calculated as the charge on each electrode by $\tilde{\phi}$ alone.

As long as the space charge effect due to the avalanche charge is negligible, we don't need to know the field produced by it. All we need is the signal charge induced on each electrode. If the boundary condition set by the electrode configuration is simple we may solve for $\tilde{\phi}$ directly. If it is not so, the reciprocal theorem comes in handy to determine the response function of each electrode. In such a case we can prepare a set of solutions for the voltage setting in which all but a-th electrode are grounded and that there is no space charge. Denoting the solution in such a case as $\hat{\phi}_a(\boldsymbol{x}; \hat{V}_a)$, we can write down the reciprocal theorem as

$$Q_a \hat{V}_a + \int d^3\boldsymbol{x}\, \tilde{\rho}(\boldsymbol{x})\, \hat{\phi}_a(\boldsymbol{x}) = 0$$

For a set of point-like charges, we have

$$\tilde{\rho}(\boldsymbol{x}) = \sum_i q_i\, \delta^3(\boldsymbol{x} - \boldsymbol{x}_i)$$

and hence

$$\hat{V}_a\, Q_a(t) + \sum_i q_i\, \hat{\phi}_a(\boldsymbol{x}_i(t)) = 0$$

Solving this for Qa, we finally obtain

$$Q_a(t) = \sum_i q_i \left(-\frac{\hat{\phi}_a(\boldsymbol{x}_i(t))}{\hat{V}_a} \right)$$

This means that the response function of a-th electrode is given by

$$F_a(\boldsymbol{x}_i) = -\frac{\hat{\phi}_a(\boldsymbol{x}_i)}{\hat{V}_a}$$

and the net charge on it by

$$Q_a(t) = \sum_i q_i\, F_a(\boldsymbol{x}_i(t))$$

Ramo's Theorem

Differentiating -Qa with respect to t, we get Ramo's theorem for outgoing current:

$$I_a(t) = -\sum_i q_i \left(\frac{\boldsymbol{E}_a(\boldsymbol{x}_i(t))}{\hat{V}_a} \cdot \dot{\boldsymbol{x}}_i(t) \right)$$

with

$$\boldsymbol{E}_a(\boldsymbol{x}) = -\nabla \hat{\phi}_a(\boldsymbol{x})$$

The signal time development is subject to the motion of the avalanche charges. The theorem shows that the contribution of an avalanche charge to the total charge collected by a-th electrode after a long

enough time is proportional to the charge times the potential difference experienced in the field "Ea". Now consider a pair of avalanche electron and its +ve ion partner which will not arrive at "a". Then they must arrive at some other electrodes with

$$\hat{V}_{b\neq a} = 0$$

The contributions of the pair hence cancel. The net charge really arriving at electrode "a" thus decides the response function. In practical applications of MPGD readout TPCs, we usually adopt such a slow enough readout scheme so as to make full use of available statistical power of primary and 2ndary ionization electrons created by an incident track.
In such a case, the net charge collected by a single electrode is determined by the size and the shape of the avalanche electron distribution when they arrive at the anode. It is, however, worth pointing out that the +ve ions mostly experience the potential difference and hence mainly contribute to the signal in the case of micromegas, while in the case of GEM, the electrons dominate the signal generation.

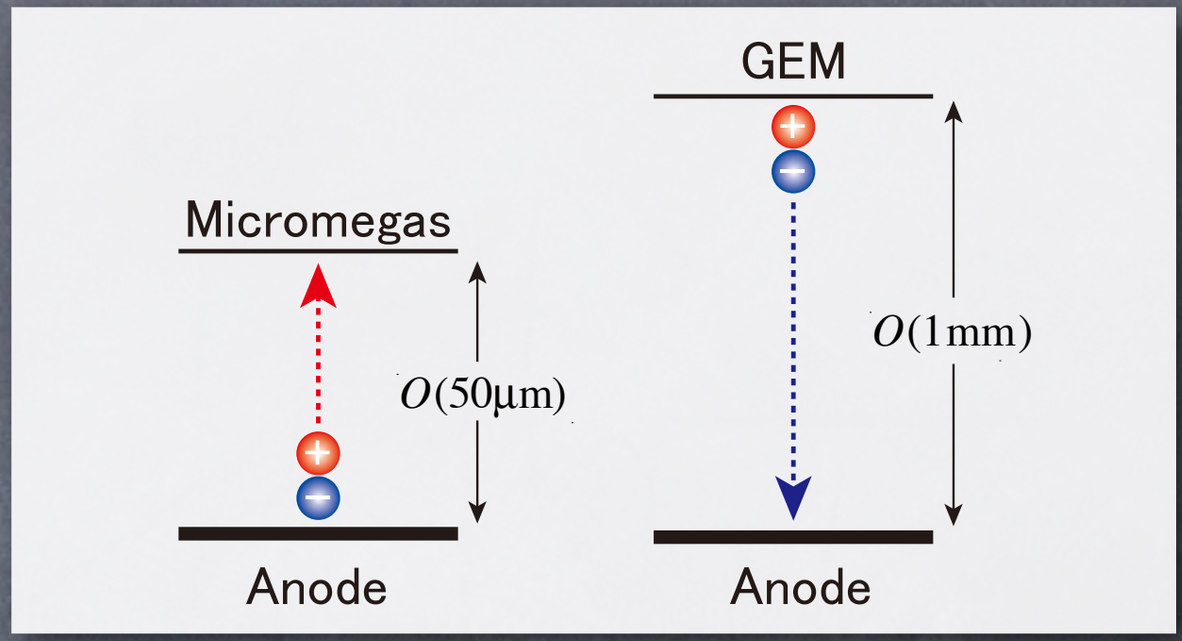

Let us investigate this in a little bit more detail below.

A Pair of Parallel Plates

A pair of parallel conductive plates is a heuristic example since it approximates the situation with a MPGD such as micromegas or GEM and that it can be easily solved by method of mirror image.

Micromegas Case

In the case of a micromegas detector, the readout anode pads are usually much larger than the avalanche size as well as than the gap length. It is hence safe to assume that a single pad is going to collect all the real charge eventually and that the induction signals on the other pads are negligible all the time. In this case we can directly apply Ramo's theorem

$$I_a(t) = -\sum_i q_i \left(\frac{\boldsymbol{E}_a(\boldsymbol{x}_i(t))}{\hat{V}_a} \cdot \dot{\boldsymbol{x}}_i(t) \right)$$

with

$$\boldsymbol{E}_a(\boldsymbol{x}) = -\nabla \hat{\phi}_a(\boldsymbol{x})$$

We can set $\hat{V}_a$ to be the voltage of the anode plane relative to the micromegas foil and assume that the foil itself is grounded. Ea is then the original amplification field:

$$\boldsymbol{E}_a = \frac{\hat{V}_a}{\Delta} \boldsymbol{e}_z$$

where Δ is the amplification gap length.

Putting this into the above eq., we obtain

$$I_a(t) = -\sum_i q_i \left(\frac{1}{\Delta} v_i(t) \right)$$

where v_i is the average velocity of i-th charge. For electrons we have

$$v^-(t) := -v_d^- \, \theta\left(t - \frac{\Delta - z_0}{v_d^-} \right) \theta\left(\frac{\Delta}{v_d^-} - t \right)$$

while for positive ions

$$v^+(t) := v_d^+ \, \theta\left(t - \frac{\Delta - z_0}{v_d^-} \right) \theta\left(\frac{\Delta - z_0}{v_d^-} + \frac{\Delta - z_0}{v_d^+} - t \right)$$

where z_0 is the z-coordinate at which the electron/ion pair is created and $v_d^{\mp}$ are the electron/ion drift velocities. We take the anode plane at z=0 and assume that the seed electron enters the amplification gap at t=0. Since most avalanche charges are created near the anode plane (say, in the last several steps) for a micromegas, the above formula tells us that its signal is mostly due to the motion of positive ions with a small but fast contribution from the electrons at the beginning.

GEM Case

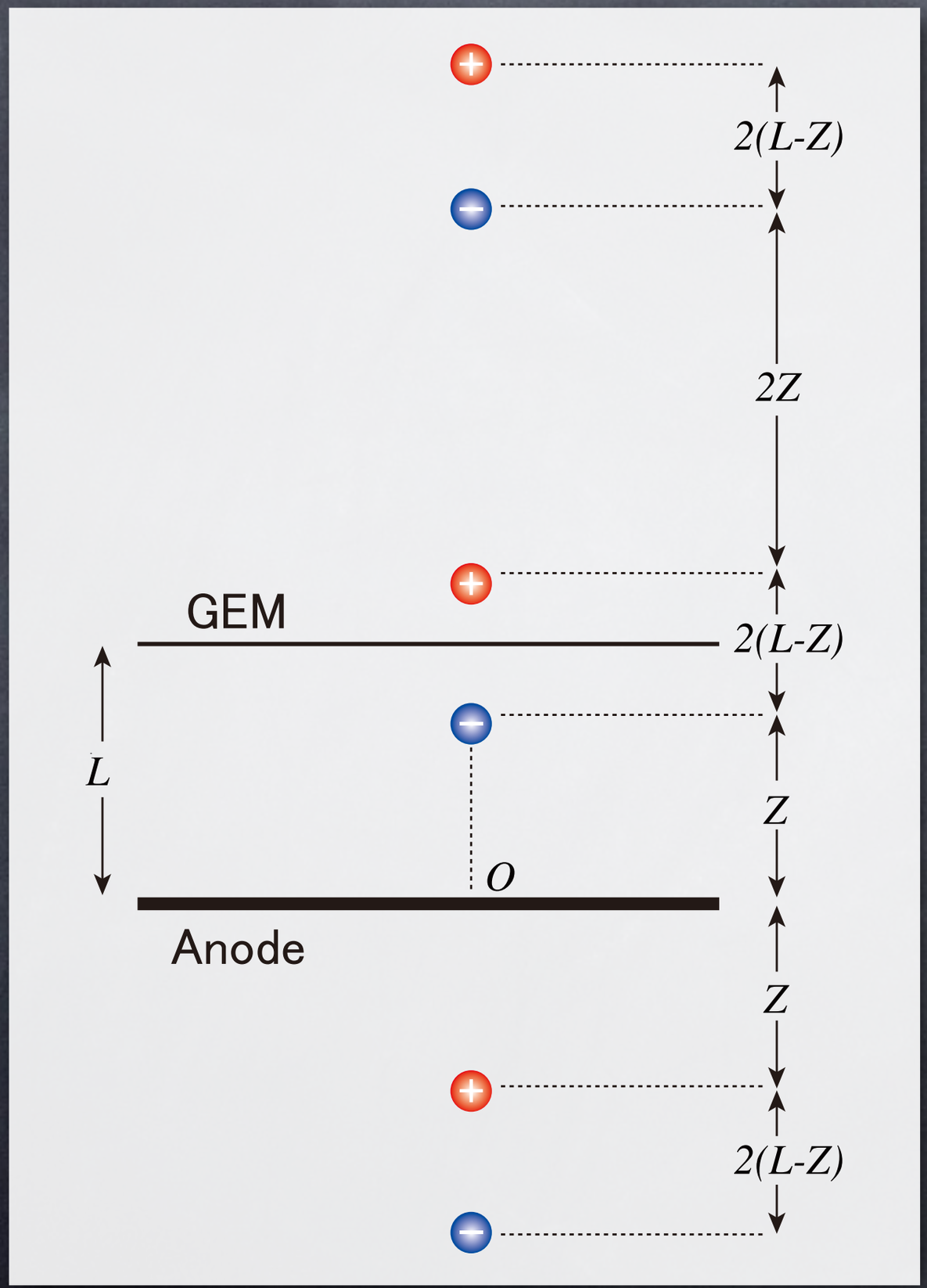

In the case of a GEM detector, the most avalanche charges are created inside the GEM holes. We can safely assume that the +ve ions stay there while the electrons are drifting towards the anode plane and hence the current signal is almost entirely due to the electrons.

We can calculate the induced signal on the anode pads by method of image. The left figure shows a few image charges together with the original one at a distance of Z from the anode. The potential is then given as the sum of the contributions from all these charges:

$$\begin{aligned}\tilde{\phi}(\boldsymbol{x}) \quad = \quad & q\sum_{k=0}^{\infty}\Bigg[\frac{1}{\sqrt{x^2+y^2+(z-(2Lk+Z))^2}} \\ & -\frac{1}{\sqrt{x^2+y^2+(z+(2Lk+Z))^2}} \\ & -\frac{1}{\sqrt{x^2+y^2+(z-(2L(k+1)-Z))^2}} \\ & +\frac{1}{\sqrt{x^2+y^2+(z+(2L(k+1)-Z))^2}}\Bigg]\end{aligned}$$

Differentiating this with respect to x on the anode plane, we can calculate the E- field there. The E-field on the anode plane can then be translated into the surface charge density

$$\rho_{\rm p}(x,y;Z) := -\frac{1}{4\pi}\left[\frac{\partial\tilde{\phi}}{\partial z}\right]_{(x,y,z;Z)=(x,y,0;Z)}$$

Integrating this over the pad in question we can get the induced signal charge:

$$Q_a(t) = \int_{D_a} da\, \rho_{\rm p}(x,y;Z(t))$$

Be careful that this is the charge flowing into the pad, the outgoing signal charge has the opposite sign.
Notice that Z(t) is given by

$$Z(t) = \theta\left(\frac{L}{v_d^-} - t\right)\left(L - \theta(t)\, v_d^-\, t\right)$$

The following figure shows the result of a sample calculation assuming an induction gap of 3mm, a pad width of 1.27mm, and a vd- of 0.05[mm/ns]. The pad height is infinite.

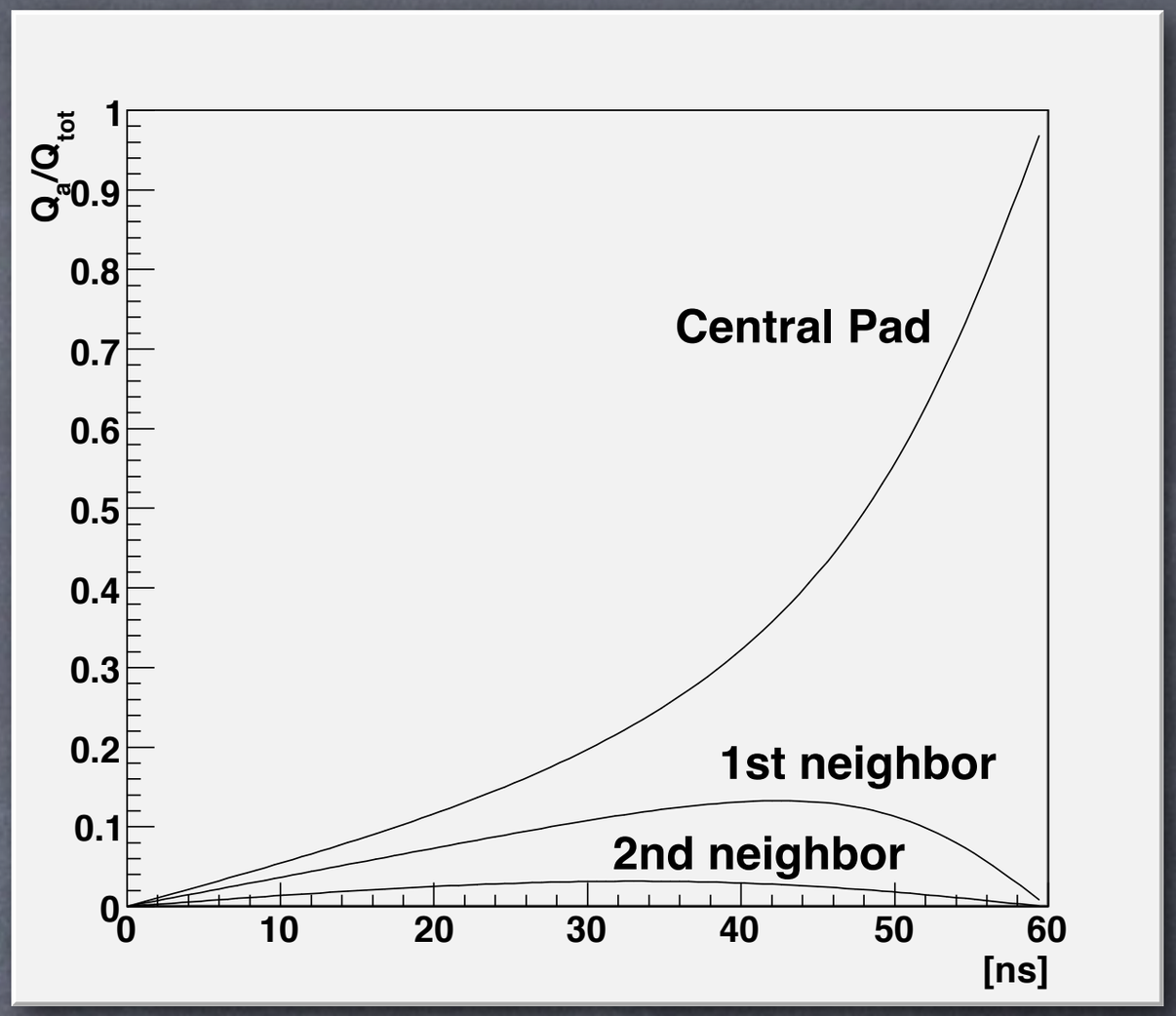

Even for a point charge, we have finite signals on side pads but they return to zero when the charge arrives at the central pad as predicted by Ramo's theorem. Of course the actual signal width in practice (with a slow readout electronics) is mostly due to the diffusion in the drift region and the transfer and the induction gaps and the projected track width.

Signals on Electrodes

In the Case of Resistive Anode

Why resistive anode?

A micromegas signal is too narrow for ordinary readout pads to benefit from the charge centroid method. The spatial resolution will be dominated by so-called hodoscope effect as we will see later. There are at least two ways out known to overcome this difficulty: (i) pixel readout matching the avalanche size; (ii) resistive anode readout to spread the signal. Option (i) can be regarded as the use of ultra fine pads, an extreme case of the conductive electrodes. Though it has a fundamental advantage to allow extracting all of the available information, there is nothing fundamentally different in terms of signal generations. We will hence concentrate on option (ii) from now on.

Although, in principle, the resistive anode is also applicable to GEMs, we assume below a micromegas detector, since the hodoscope effect is more prominent for it.
The structure of the resistive anode is shown below.

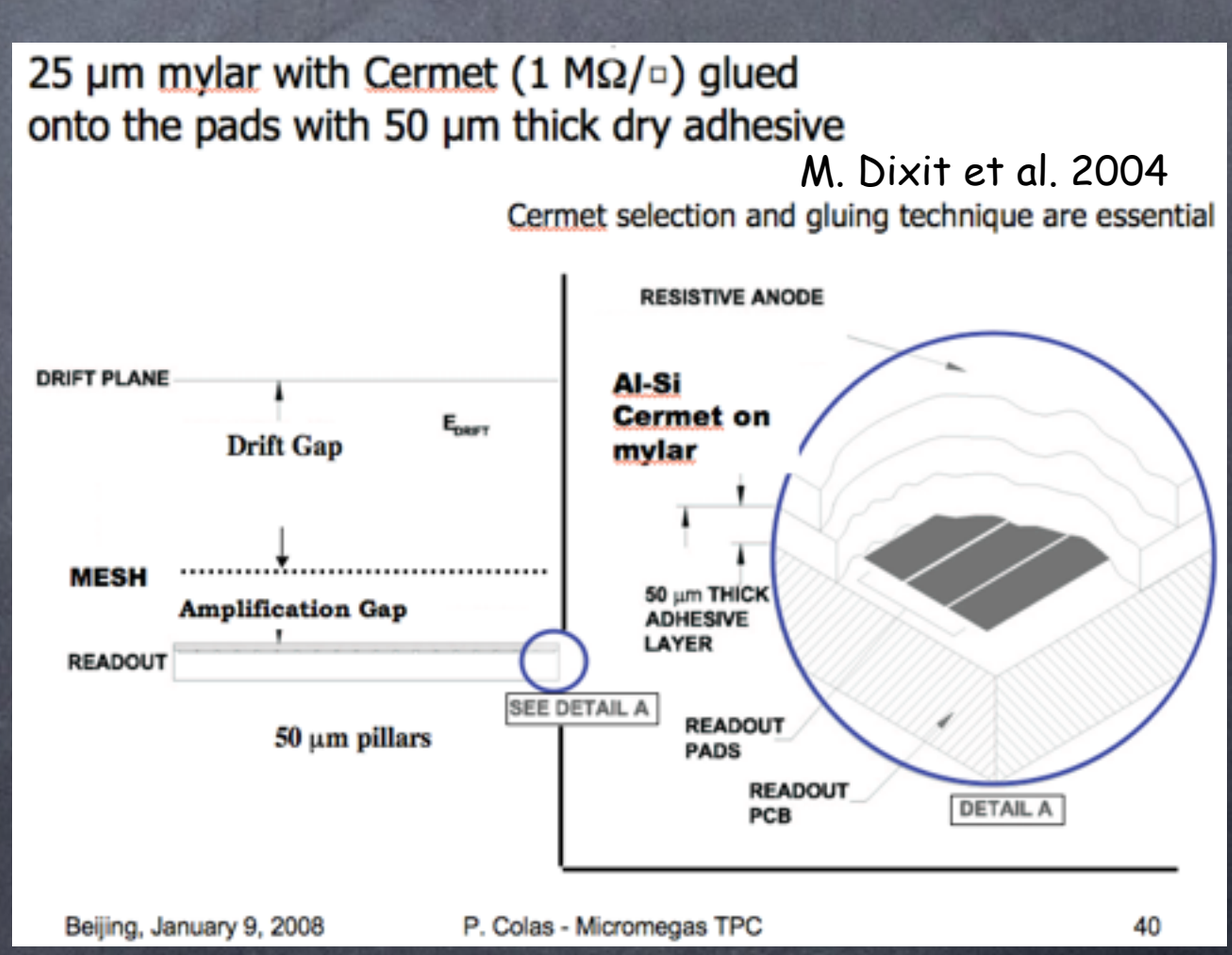

Signal Generation Process

If the resistive anode has a high enough surface resistance, it will be transparent for the E-field created by the quick motion of the avalanche charges while they are drifting in the gas. The signal on each electrode below the resistive foil will be the same as with conductive electrodes alone. We hence consider here the signal development after the avalanche electrons arriving at the surface of the resistive foil.

The avalanche electrons then propagate along the surface of the resistive foil while inducing a mirror charge on the pad plane. Let us now derive the equation for the time development of the induced charge on the pad plane. We assume here that the gap between the resistive foil and the pad plane is small enough that the induced electric field is confined between this gap. Now consider a small cylinder (see (a) in the next figure) and apply the Gauss law to it.

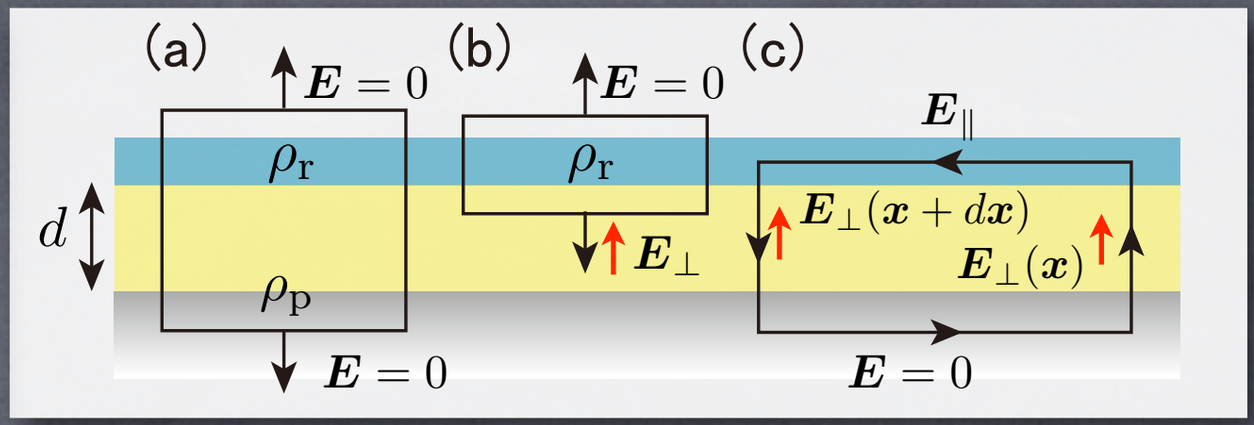

Since there is no field above the resistive foil and in the pad plane and the field is nearly parallel with the side wall, we obtain

$$0 = \int_{\partial(a)} d\boldsymbol{a}\cdot\epsilon\boldsymbol{E} = 4\pi(\rho_{\mathrm{r}}+\rho_{\mathrm{p}})\,da$$

where we have introduced surface charge densities on the resistive foil and the pad plane:

$$\rho = \rho_{\mathrm{r}}(x,y;t)\delta(z-d) + \rho_{\mathrm{p}}(x,y;t)\delta(z)$$

We hence have a mirror relation expected for the thin (small d) insulator layer:

$$\rho_{\mathrm{p}} = -\rho_{\mathrm{r}}$$

Similarly if we apply the Gauss law to (b), we have

$$-\epsilon E_\perp\,da = \rho_{\mathrm{r}}\,da$$

leading us to

$$E_\perp = -\frac{1}{\epsilon}\rho_{\mathrm{r}}$$

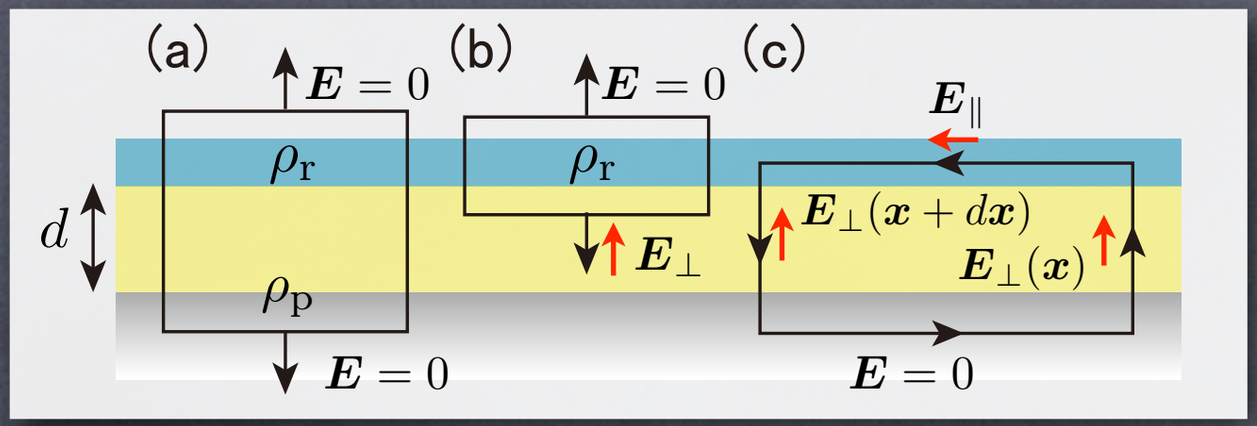

Let us now consider a loop shown in (c). If we surface-integrate the Faraday law over the area surrounded by this loop, we have

$$\boldsymbol{E}_\parallel \cdot d\boldsymbol{x} - (E_\perp(\boldsymbol{x}+d\boldsymbol{x}) - E_\perp(\boldsymbol{x}))\; d = 0$$

where we have ignored the magnetic flux passing through the loop. Taylor-expanding the 2nd term on the L.H.S. we have

$$\boldsymbol{E}_\parallel - d\,\frac{\partial}{\partial \boldsymbol{x}} E_\perp = 0$$

Recalling

$$E_\perp = -\frac{1}{\epsilon}\rho_{\rm r}$$

we obtain

$$\boldsymbol{E}_\parallel = -\frac{d}{\epsilon}\,\frac{\partial}{\partial \boldsymbol{x}}\rho_{\rm r}$$

The current on the resistive foil should be proportional to this parallel field

$$\boldsymbol{J}_{\rm r} = \sigma\,\delta(z-d)\boldsymbol{E}_\parallel$$

where the sigma is the conductivity of the resistive foil times the foil thickness which is assumed to be negligible. Putting these into the charge conservation law (continuity eq.) for the resistive foil

$$0 = \frac{\partial}{\partial t}\rho_{\rm r}\,\delta(z-d) + \frac{\partial}{\partial \boldsymbol{x}}\cdot\boldsymbol{J}_{\rm r}$$

and canceling out the delta function, we get

$$\frac{\partial}{\partial t}\rho_{\rm r} - \left(\frac{\sigma\, d}{\epsilon}\right)\triangle_2\,\rho_{\rm r} = 0$$

where $\triangle_2$ is the 2-dimensional Laplacian.

Introducing the capacitance per unit area (C) and the resistance per square area (R)

$$C := \frac{\epsilon}{d} \qquad \text{and} \qquad R := \frac{1}{\sigma}$$

and noting the mirror relation

$$\rho_{\rm p} = -\rho_{\rm r}$$

we finally arrive at the telegraph equation:

$$\frac{\partial}{\partial t}\,\rho_{\rm p} - \left(\frac{1}{RC}\right)\triangle_2\,\rho_{\rm p} = 0$$

This is none other than a 2-dim. diffusion eq. which has a Gaussian solution for a point

charge initial condition

$$\rho_{\rm p}(r;t_0) = \frac{q}{2\pi r}\delta(r)$$

as we have seen in treating transportation of electrons in a gas:

$$\rho_{\rm p}(r;t) = \frac{q}{2\pi\sigma_{\rm p}^2}\, e^{-\frac{r^2}{2\sigma_{\rm p}^2}}$$

where

$$r := \sqrt{(x-x_0)^2+(y-y_0)^2}$$

and

$$\sigma_{\rm p}^2 := \frac{2}{RC}(t-t_0)$$

Notice that the Gaussian width is decided by a single parameter "RC" and the elapse time. By integrating this Gaussian over a readout pad, we can calculate the induced charge on it as a function of time.
Notice that the telegraph equation, being homogeneous, obeys superposition principle. The net signal is thus obtained by summing over all the avalanches arriving at different (x0, y0)'s and at different t0's.

For R=1MOhm/sqare and C=1pF/pad, gives a RC value of 1 micro second/pad area, meaning that after about 1 micro second a point charge spreads over a pad size. The following figure shows expected signals on pads about the avalanche:

M. Dixit

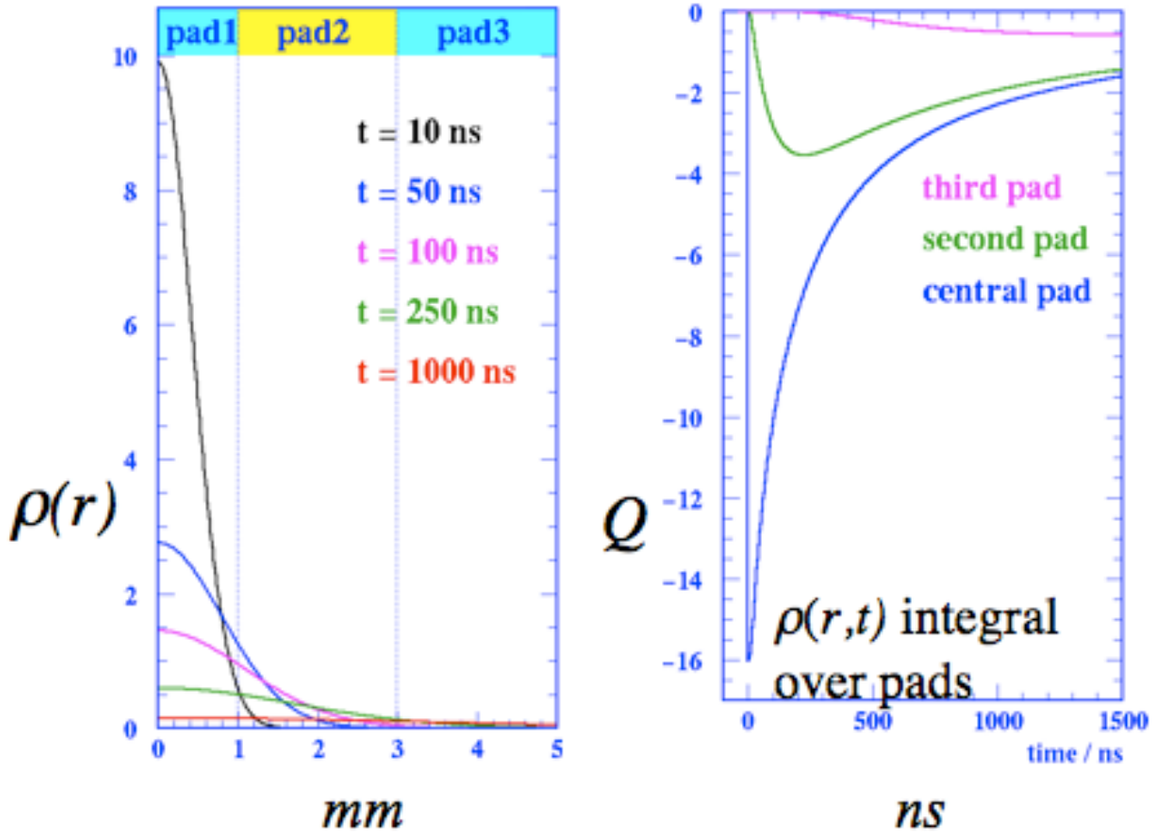

In practice, the signal width is determined by the convolution of this and the spread due to the diffusion of seed electrons in the drift region as well as the track width.

Basic Physics Behind Operation of TPC

Part II

-- Application to MPGD Readout TPCs --

Keisuke Fujii

iSTEP 2014, IHEP Beijing, Aug. 2014

Coordinate Measurements

Charge Centroid Method with Readout Pads

Fundamental Limits on Spatial Resolution
for a MPGD Readout TPC

Analytic Formulation of Spatial Resolution
Important Outcome from KEK Beam Tests
(Asia, Europe, and North America)

MPGD Readout TPC

Coordinate Measurement Process

Coordinate System

We set our coordinate system in such a way that the readout pads are arranged in a row to measure the x-coordinate with charge centroid method, the y-coordinate from the pad row number, and the z-coordinate from the drift time.

Basic Assumptions

For simplicity, we will consider for a while a charged particle at normal incidence. We also assume that the effect of delta-rays is negligible (good approximation if there is a strong enough B-field) so that all the track electrons can be regarded as starting from a single point when projected to the (x, z) plane. These track electrons drift towards the amplification region while experiencing diffusion. The track electrons are then gas amplified while experiencing further diffusion. As we have discussed, when we readout pad signals with a slow enough electronics, only the real charge arriving at a readout pad counts. The spatial width of the signal is then determined by the width of the real charge distribution on the pad plane as determined by the diffusion in the drift and the amplification regions. Notice that we are dealing with normal incidence for which angular pad effect is absent.

In what follows we start from an ideal situation with a perfect readout plane, switching on one-by-one complications expected for more realistic situations.

Fundamental Processes

Beam

Ionizations

⟶ Liberation of Electrons

$P_I(N;\bar{N})$ Normal incidence (no angle effect)

No δ-ray

Drift Volume

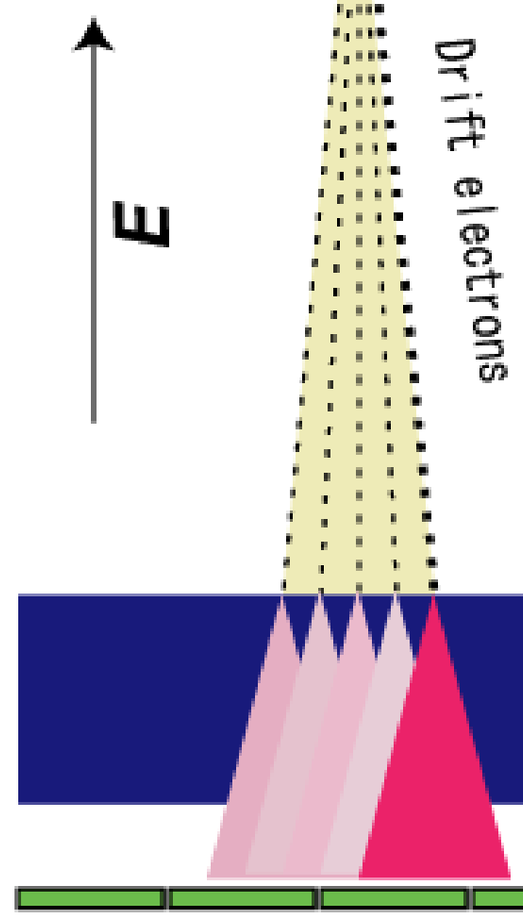

Drift and Diffusion

$$P_D(x_i;\sigma_d) = \frac{1}{\sqrt{2\pi}\sigma_d}\exp\left(-\frac{x_i^2}{2\sigma_d^2}\right)$$

$$\sigma_d = C_d\sqrt{z}$$

Amplification Gap

Amplification and further Diffusion

Readout Pads

$$P_G(G/\bar{G};\theta) = \frac{(\theta+1)^{\theta+1}}{\Gamma(\theta+1)}\left(\frac{G}{\bar{G}}\right)^{\theta}\exp\left(-(\theta+1)\left(\frac{G}{\bar{G}}\right)\right)$$

Pad Response

Coordinate

Ionization Statistics

Ideal Readout Plane: Coordinate = Simple C.O.G.

PDF for C.O.G. of N electrons

We assume here an ideal readout plane that can measure the x-coordinates of individual track electrons exactly. The probability distribution function for the center of gravity of N track electrons is given by

$$P(\bar{x}) = \sum_{N=1}^{\infty} P_I(N;\bar{N}) \prod_{i=1}^{N} \left(\int dx_i \, P_D(x_i;\sigma_d) \right) \delta\left(\bar{x} - \frac{1}{N} \sum_{i=1}^{N} x_i \right)$$

Ionization statistics

Ideal readout plane

Gaussian diffusion

$$P_D(x_i;\sigma_d) = \frac{1}{\sqrt{2\pi}\sigma_d} \exp\left(-\frac{x_i^2}{2\sigma_d^2} \right)$$

$$\sigma_d = C_d \sqrt{z}$$

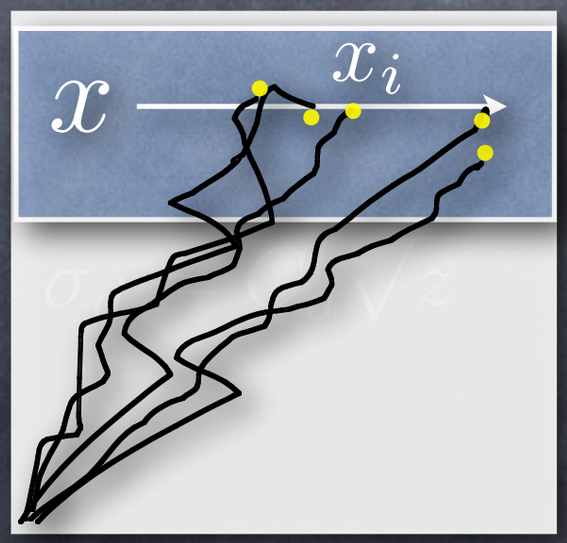

where Cd is the diffusion coefficient and z is the drift length. The track is assumed to passed through the TPC at x=0 parallel with the readout plane and perpendicular to the pad rows.

The center of gravity of the N electrons is the best possible estimator of the incident x-coordinate of the track

$$\langle \bar{x} \rangle := \int d\bar{x} \, P(\bar{x}) \, \bar{x} = 0$$

The variance of the C.O.G. is then given by

$$\sigma_{\bar{x}}^2 := \int d\bar{x} \, P(\bar{x}) \, \bar{x}^2 = \sigma_d^2 \left\langle \frac{1}{N} \right\rangle =: \sigma_d^2 \frac{1}{N_{\text{eff}}}$$

by definition. This leads us to

$$N_{\text{eff}} := \frac{1}{\langle 1/N \rangle} < \langle N \rangle$$

What decides the spatial resolution is not the average number of ionization electrons but the inverse of the average of its inverse.

Gas Gain Fluctuation

Coordinate = Gain-Weighted Mean

PDF for gain-weighted mean

We now switch on the gas gain fluctuation and assume that the coordinate measured by the readout plane is the gain-weighted mean of the N ionization electrons.

$$P(\bar{x}) = \sum_{N=1}^{\infty} P_I(N;\bar{N}) \prod_{i=1}^{N} \left[\int dx_i \, P_D(x_i;\sigma_d) \times \int d\left(\frac{G_i}{\bar{G}}\right) P_G\left(\frac{G_i}{\bar{G}};\theta_{\rm pol}\right) \right] \delta\left(\bar{x} - \frac{\sum_{i=1}^{N} G_i \, x_i}{\sum_{i=1}^{N} G_i} \right)$$

Gas gain fluctuation

Gain-weighted mean

We used the Polya parameter as an index even though the PG is non-Polya in general. Notice that

$$\sum_{i=1}^{N} G_i \approx N \, \bar{G}$$

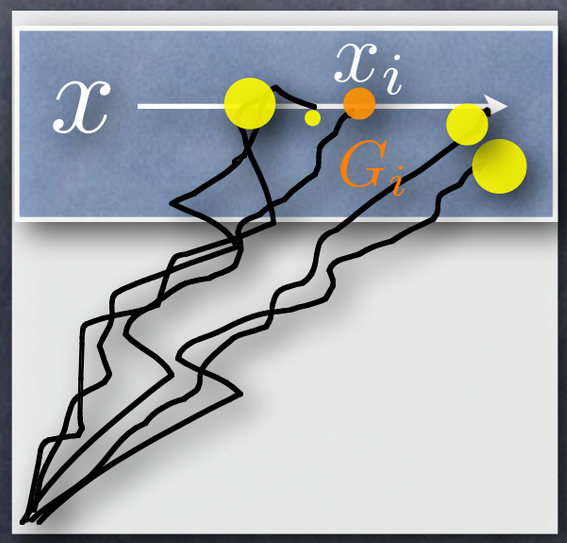

Again we assume that the charged particle passed through the TPC at x=0 parallel with the readout plane and perpendicular to the pad rows.

The average of the gain-weighted mean has then no bias

$$\langle \bar{x} \rangle := \int d\bar{x} \, P(\bar{x}) \, \bar{x} = 0$$

The variance of the C.O.G. is then given by

$$\sigma_{\bar{x}}^2 := \int d\bar{x} \, P(\bar{x}) \, \bar{x}^2 \approx \sigma_d^2 \left\langle \frac{1}{N} \right\rangle \left\langle \left(\frac{G}{\bar{G}} \right)^2 \right\rangle =: \sigma_d^2 \frac{1}{N_{\rm eff}}$$

where use has been made of

$$\sum_{i=1}^{N} G_i \approx N \, \bar{G}$$

We hence have

$$N_{\rm eff} := \left[\left\langle \frac{1}{N} \right\rangle \left\langle \left(\frac{G}{\bar{G}} \right)^2 \right\rangle \right]^{-1} = \frac{1}{\langle 1/N \rangle} \left(\frac{1+\theta_{\rm pol}}{2+\theta_{\rm pol}} \right) < \langle N \rangle$$

The gas gain fluctuation therefore further reduces the effective number of electrons.

Sample Calc. for Neff

For 4 GeV pion and pad row pitch of 6mm in pure Ar

M.Kobayashi

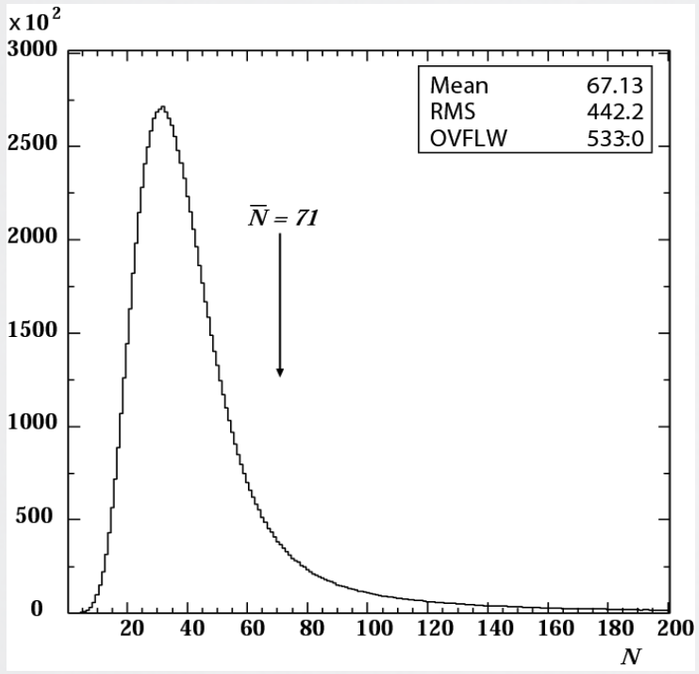

Distribution of *N*
(<*N*> = 71)

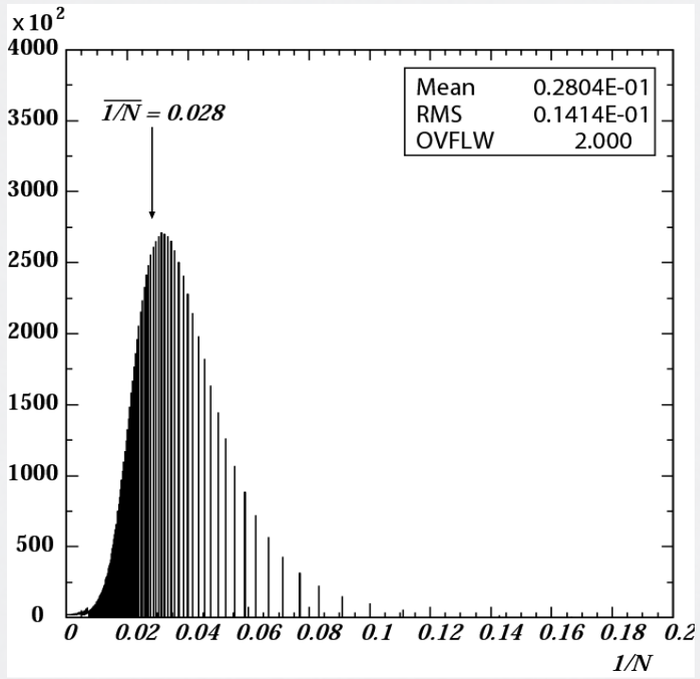

Distribution of 1/*N*
(<1/*N*> = 0.028)

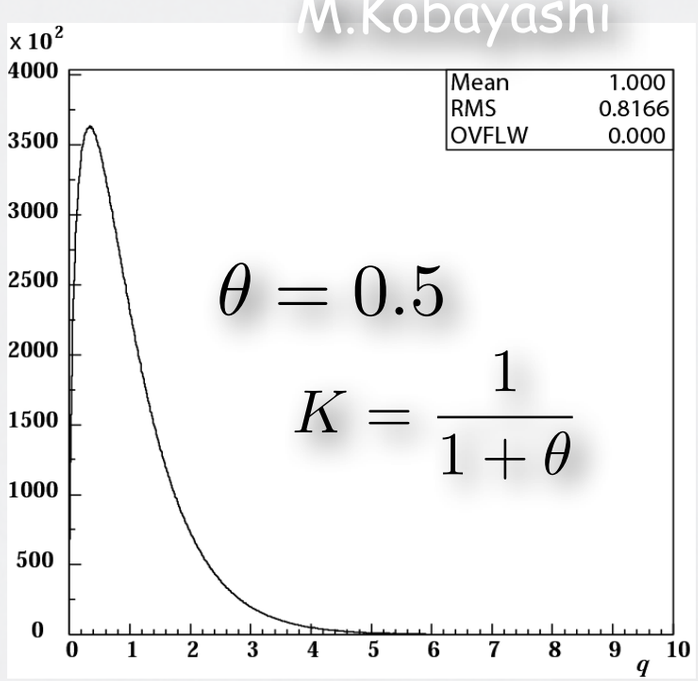

Distribution of *Q*
(*K* = 0.67)

In the case of Snyder's model, gain fluctuation is exponential and K=1 (theta=0) and the Neff is reduced by a factor of 2 by it. In the case of Legler's model, theta>0 and the reduction is less sever. If we assume theta=0.5, for instance, we have a factor of 1.5 reduction:

$$N_{eff} = \left[\left\langle \frac{1}{N} \right\rangle \left\langle \left(\frac{G}{\bar{G}}\right)^2 \right\rangle\right]^{-1} = 21 < \langle N \rangle = 71$$

$$\left\langle \left(\frac{G}{\bar{G}}\right)^2 \right\rangle = 1 + \left(\frac{\sigma_G}{\bar{G}}\right)^2 \equiv 1 + K$$

Finite Size Pads

Coordinate = Charge Centroid

PDF for charge centroid

We now replace the continuous readout plane with an array of finite size pads.
The finite size pads break the translational symmetry. We hence need to specify the track position relative to the pad center. The arrival point of i-th ionization electron is given by

diffusion : $\langle (\Delta x_i)^2 \rangle = \sigma_d^2 = C_d^2 \, z$

$$x_i = \tilde{x} + \Delta x_i$$

track position

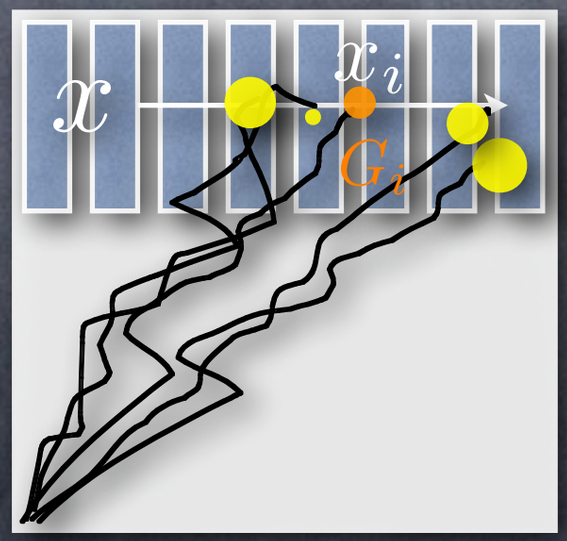

The charge in units of electron charge on a-th pad is given by

$$Q_a = \sum_{i=1}^{N} G_i \, F_a(\tilde{x} + \Delta x_i) + \Delta Q_a$$

where F_a is the normalized pad response function for a-th pad

$$\sum_a F_a(\tilde{x} + \Delta x_i) = 1$$

G_i is the gas gain for the i-th ionization electron, and ΔQ_a is the electronic noise:

$$\langle (\Delta Q_a)^2 \rangle = \sigma_E^2$$

The charge centroid is then given by

$$\bar{x} = \sum_a Q_a \, (a\, w) \, / \sum_a Q_a$$

with w being the pad pitch. The probability distribution function for charge centroid is

$$P(\bar{x};\tilde{x}) = \sum_{i=1}^{\infty} P_I(N;\bar{N}) \prod_{i=1}^{N} \left[\int d\Delta x_i \, P_D(\Delta x_i;\sigma_d) \int d\left(\frac{G_i}{\bar{G}}\right) P_G\left(\frac{G_i}{\bar{G}};\theta_{\rm pol}\right) \right]$$
$$\times \prod_a \left[\int d\Delta Q_a \, P_E(\Delta Q_a;\sigma_E) \int dQ_a \, \delta\left(Q_a - \sum_{i=1}^{N} G_i \, F_a(\tilde{x} + \Delta x_i) - \Delta Q_a \right) \right]$$
$$\times \, \delta\left(\bar{x} - \frac{\sum_a Q_a \, (a\, w)}{\sum_a Q_a} \right)$$

Variance of charge centroid

In order to take into account the effect of finite size pads as known as the S-shape systematics, we define the variance by

$$\sigma_{\bar{x}}^2 := \int_{-\frac{1}{2}}^{+\frac{1}{2}} d\left(\frac{\tilde{x}}{w}\right) \int d\bar{x}\, P(\bar{x};\tilde{x})\,(\bar{x}-\tilde{x})^2$$

Substituting the PDF given above in this and with some arithmetics, we obtain

$$\sigma_{\bar{x}}^2 = \int_{-\frac{1}{2}}^{+\frac{1}{2}} d\left(\frac{\tilde{x}}{w}\right) \left[[A] + \frac{1}{N_{\rm eff}}[B]\right] + [C]$$

where

$$[A] := \left(\sum_a (a\,w)\,\langle F_a(\tilde{x}+\Delta x)\rangle - \tilde{x}\right)^2$$

is a purely geometric term corresponding to the S-shape systematics due to the finite pad pitch and disappears rapidly as z increases. On the other hand,

$$[B] := \sum_{a,b} a\,b\,w^2\,\langle F_a(\tilde{x}+\Delta x)F_b(\tilde{x}+\Delta x)\rangle - \left(\sum_a a\,w\,\langle F_a(\tilde{x}+\Delta x)\rangle\right)^2$$

is a term representing the contributions from diffusion, gas gain fluctuation, and finite pad pitch. The contribution of this term scales as 1/Neff and dominates the spatial resolution at a long drift distance.
The last term

$$[C] := \left(\frac{\sigma_E}{\bar{G}}\right)^2 \left\langle \frac{1}{N^2} \right\rangle \sum_a (a\,w)^2$$

is an electronic noise term, which is z-independent and scales as $\langle 1/N^2 \rangle$

The correlation function and the averaged pad response functions are defined by

$$\langle F_a(\tilde{x}+\Delta x)F_b(\tilde{x}+\Delta x)\rangle := \int d\Delta x\, P_D(\Delta x;\sigma_d)\, F_a(\tilde{x}+\Delta x)\, F_b(\tilde{x}+\Delta x)$$

and

$$\langle F_a(\tilde{x}+\Delta x)\rangle := \int d\Delta x\, P_D(\Delta x;\sigma_d)\, F_a(\tilde{x}+\Delta x)$$

An asymptotic form at large z reads

$$\sigma_{\bar{x}}^2 \simeq \sigma_0^2 + \frac{1}{N_{eff}} C_d^2\, z$$

with

$$\sigma_0^2 := \frac{1}{N_{\rm eff}} \left[\int_{-\frac{1}{2}}^{+\frac{1}{2}} d\left(\frac{\tilde{x}}{w}\right) [A](z=0)\right] + [C]$$

Interpretation

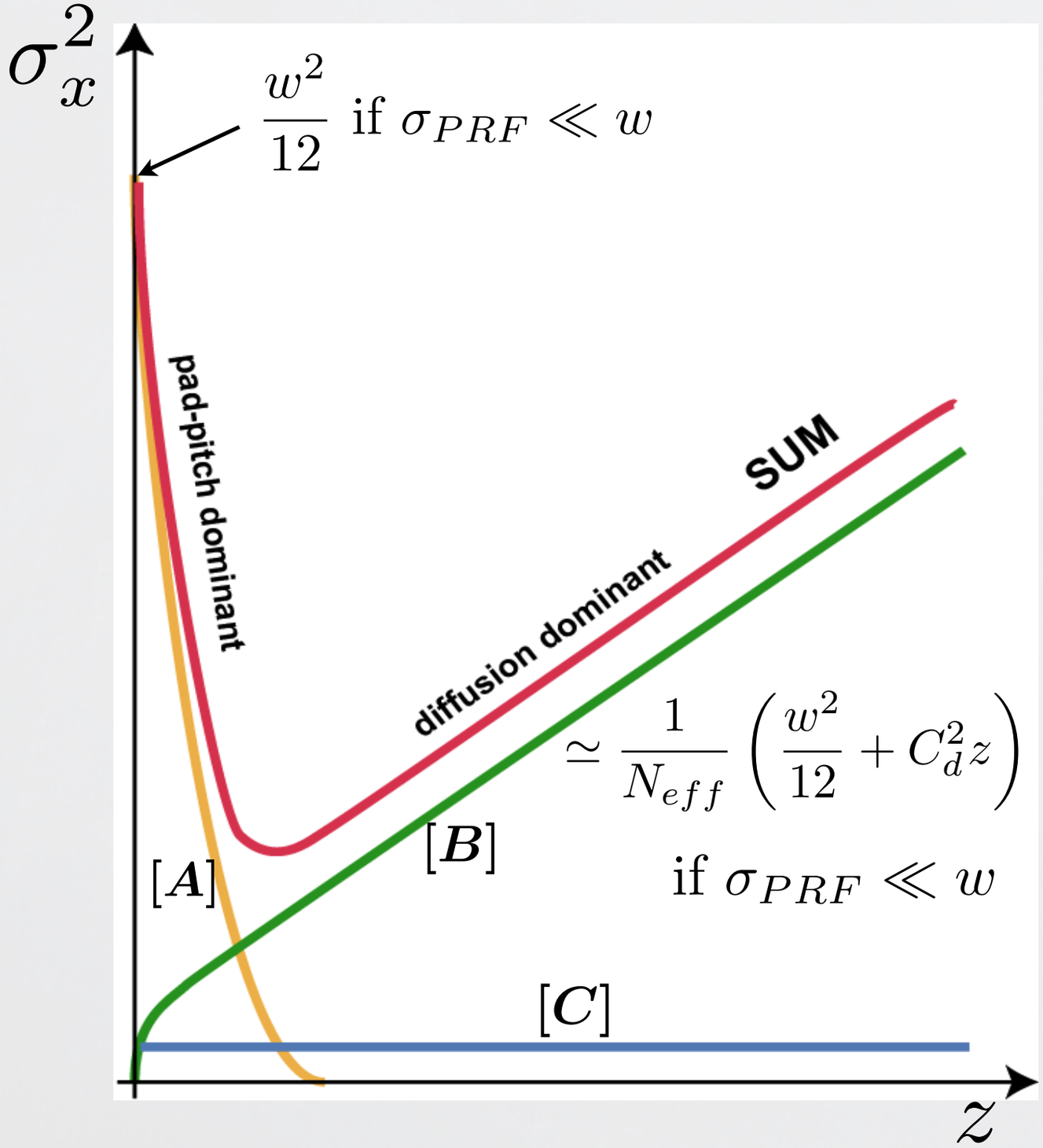

[A] Purely geometric term (S-shape systematics from finite pad pitch): rapidly disappears as Z increases

[B] Diffusion, gas gain fluctuation & finite pad pitch term: scales as $:1/N_{eff}$

$$\sigma_{\tilde{x}}^2 \simeq \frac{1}{N_{eff}} \left[\int_{-\frac{1}{2}}^{+\frac{1}{2}} d\left(\frac{\tilde{x}}{w}\right) [A](z=0) + C_d^2 \, z \right]$$

For delta-fun like PRF asymptotically:

$$\sigma_{\tilde{x}}^2 \simeq \frac{1}{N_{eff}} \left(\frac{w^2}{12} + C_d^2 z \right)$$

[C] Electronic noise term: Z-independent, scales as $\langle 1/N^2 \rangle$

Application to Micromegas

- For a delta-function like PRF, there is a scaling law: σ_x/w depends only on σ_d/w and N_{eff}
- The formula has a fixed point

$$(0, 1/\sqrt{12})$$

- Full formula enters asymptotic region at

$$\sigma_d/w \simeq 0.4$$

- Full formula has a minimum of

at

$$\sigma_x/w \simeq 0.1$$

$$\sigma_d/w \simeq 0.3$$

$(0, 1/\sqrt{12})$: hodoscope limit

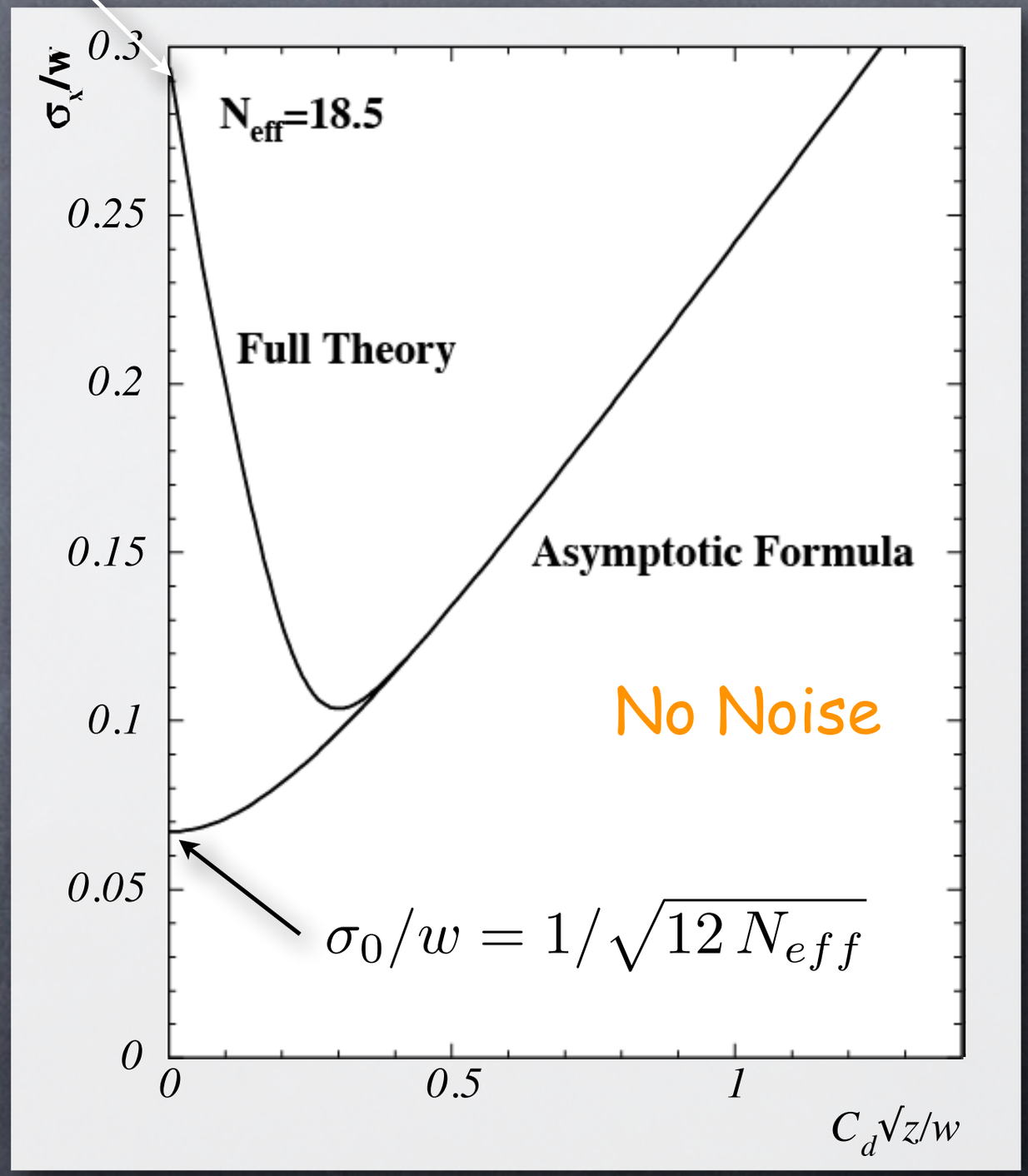

Comparison with MC

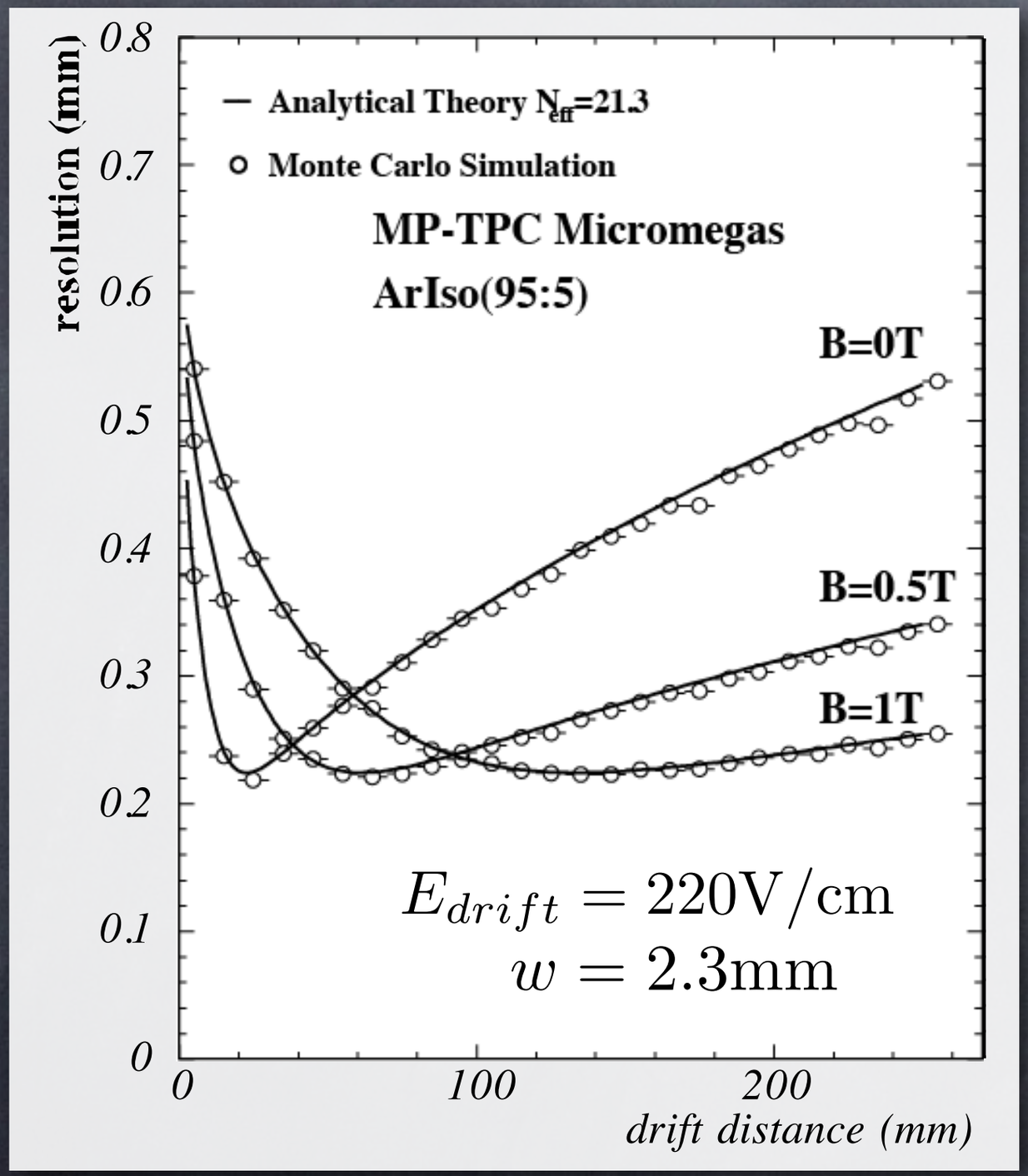

- Theory reproduces the Monte Carlo simulation very well !
- We can estimate the resolution analytically

drift distance

$$\sigma_x = \sigma_x(z; w, C_d, N_{eff}, [f_j])$$

pad pitch

diffusion const.

pad response function

δ-fun. for MM: $\sigma_{PRF} \simeq 12\mu\mathrm{m}$

gauss. for GEM: $\sigma_{PRF} \simeq 350\mu\mathrm{m}$

Comparison with Measurements

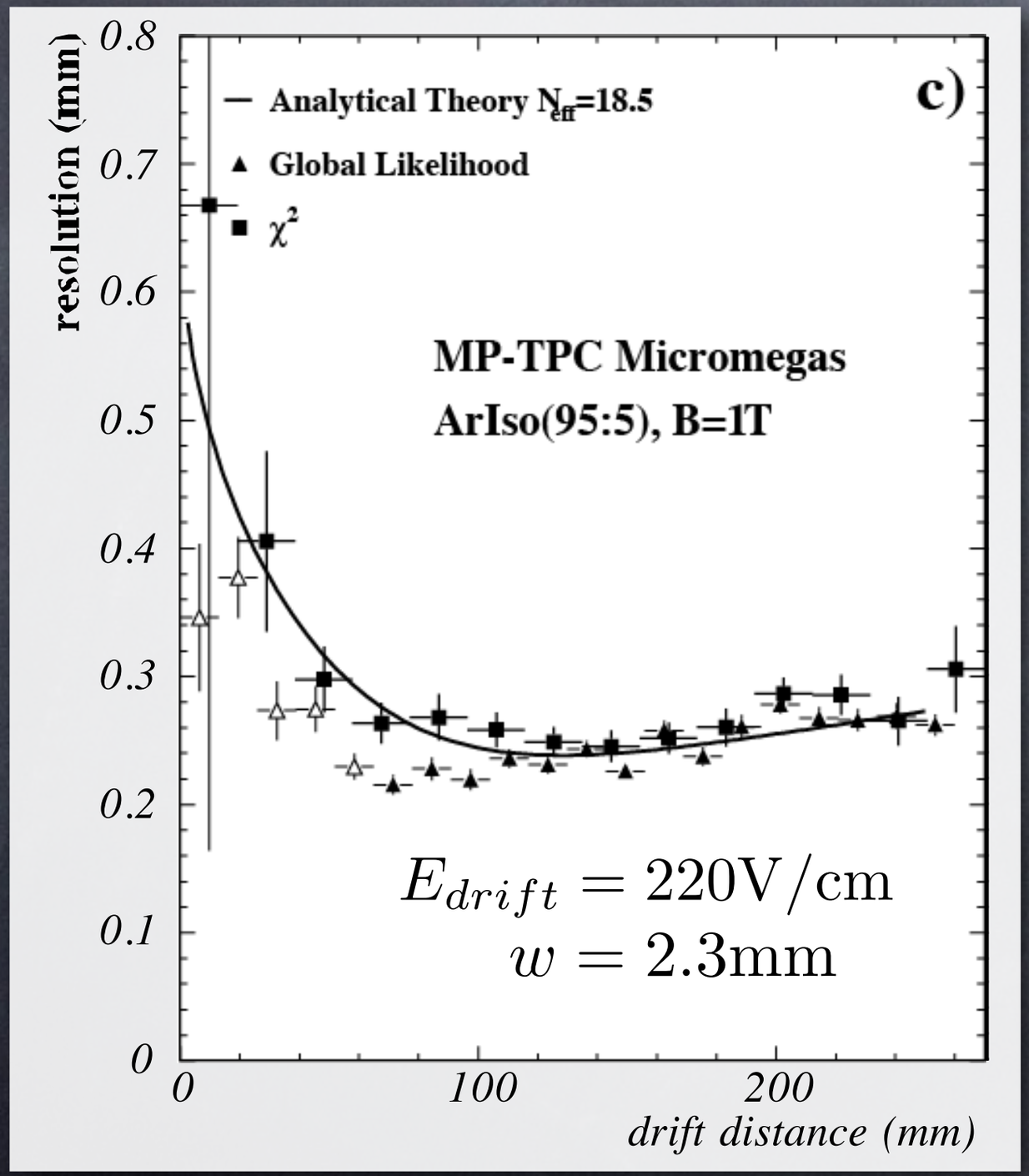

KEK beam test data

- Theory reproduces the data well.
- Underestimation in the data of σ_x at short drift distance is due to track bias caused by S-shape systematics.
- Global likelihood method eliminates the S-shape systematics at short distance when possible and hence gives better resolution than the simple charge centroid method used in the chi-square fit.

Extrapolation to LC TPC

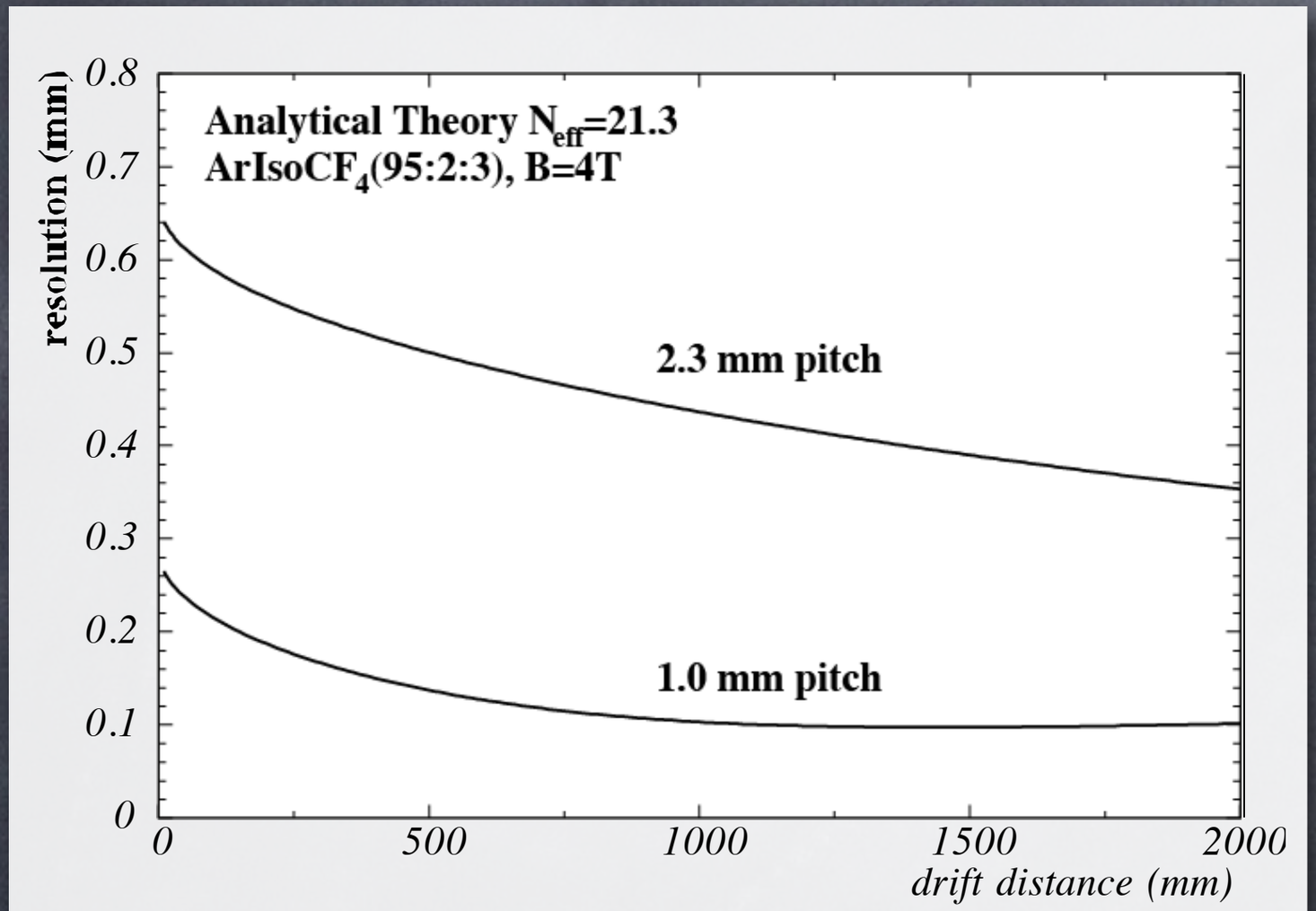

- Need to reduce pad size relative to PRF
  - Resistive anode for MM.
  - Digital pixel readout for MM corresponding to an ideal readout plane to avoid the effect of gain fluctuation (the best if feasible).
  - Defocusing + narrow (1mm) pad for GEM.

Recent results seem promising for both resistive anode and digital pixel readout schemes (Paul's talk)!

Application to GEM

TU-TPC test at KEK cryo hall (Dec. 2007)

- In the case of GEM, there is no simple scaling as with micromegas, since there is an additional dimensionful parameter that is the intrinsic signal width ($\sigma_{\rm PRF}$) which is determined by the diffusion in the transfer and induction gaps. When it is large enough compared with the pad pitch we can avoid the hodoscope effect at a short drift distance.

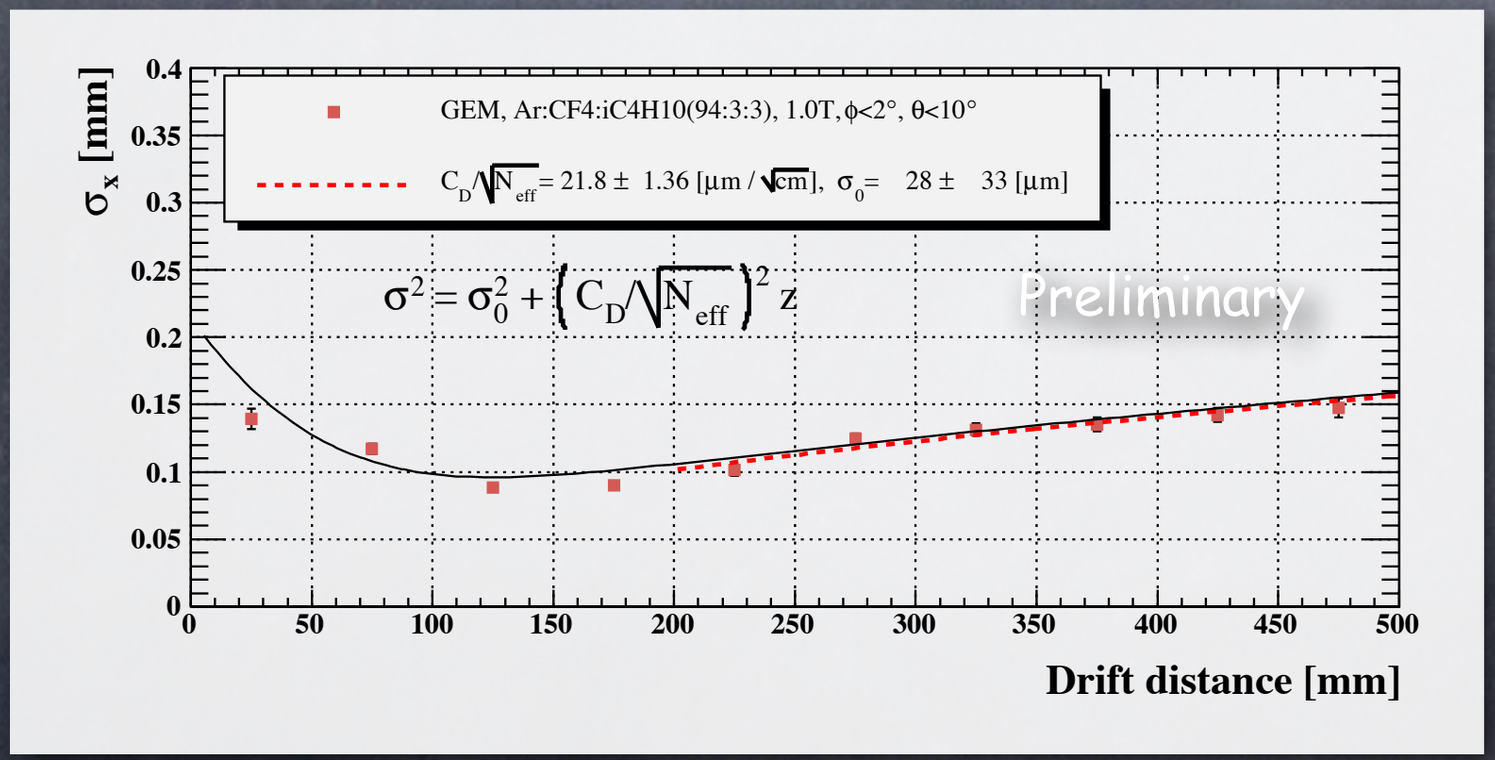

The theory assumes

$$v_{drift} = 4.2\,[\mathrm{cm}/\mu\mathrm{s}]$$

from drift time data and

$$\begin{aligned}\sigma_{PRF}^2 &= \sigma_{PR}(0)^2 - \frac{w^2}{12} \\ &= (270\,[\mu\mathrm{m}])^2\end{aligned}$$

$$C_D = 128\,[\mu\mathrm{m}/\sqrt{\mathrm{cm}}]$$

from charge width data and

$$N_{eff} = 22 \times (10./6.3) = 35$$

from MP-TPC result.

The TU-TPC data indicates

$$N_{eff} = (128/22) = 34 \pm 4$$

in good agreement with the MP-TPC result.

How to Measure Cd?

A detour

The average charge on a-th pad

The average charge on a-th pad is given by

$$\langle Q_a(\tilde{x})\rangle = \bar{N}\bar{G}\,\langle F_a(\tilde{x}+\Delta x)\rangle$$

resulting in the average charge fraction

$$\begin{aligned}
\langle Q_a(\tilde{x})\rangle/(\bar{N}\bar{G}) &= \langle F_a(\tilde{x}+\Delta x)\rangle \\
&:= \int d\Delta x\, P_D(\Delta x;\sigma_d)\, F_a(\tilde{x}+\Delta x) \\
&= \int_{a\,w-\tilde{x}-w/2}^{a\,w-\tilde{x}+w/2} d\Delta x\, \frac{1}{\sqrt{2\pi}\sigma}\exp\left[-\frac{1}{2}\left(\frac{\Delta x}{\sigma}\right)^2\right] \\
&= \int_{-w/2}^{+w/2} d\xi\, \frac{1}{\sqrt{2\pi}\sigma}\exp\left[-\frac{1}{2}\left(\frac{\hat{x}+\xi}{\sigma}\right)^2\right]
\end{aligned}$$

where

$$\hat{x} := a\,w - \tilde{x}$$

is the location of the pad center measured from the incident position of the track and

$$\sigma^2 := \sigma^2_{\rm PRF} + \sigma^2_d = \sigma^2_{\rm PRF} + C_d^2\, z$$

is the squared sum of the intrinsic width of the pad response function at z=0 and the width due to diffusion in the drift region. We can hence define a normalized apparent pad response function

$$Q_{\rm PR}(\hat{x}) := \frac{1}{w}\int_{-w/2}^{+w/2} d\xi\, \frac{1}{\sqrt{2\pi}\sigma}\exp\left[-\frac{1}{2}\left(\frac{\hat{x}+\xi}{\sigma}\right)^2\right]$$

which has the variance

$$\begin{aligned}
\sigma^2_{\rm PR} &= \int d\hat{x}\, Q_{\rm PR}(\hat{x})\,\hat{x}^2 \\
&= \frac{1}{w}\int_{-w/2}^{+w/2} d\xi \int_{-\infty}^{+\infty} d\hat{x}\, \frac{1}{\sqrt{2\pi}\sigma}\exp\left[-\frac{1}{2}\left(\frac{\hat{x}+\xi}{\sigma}\right)^2\right]\hat{x}^2 \\
&= \frac{1}{w}\int_{-w/2}^{+w/2} d\xi\,(\sigma^2+\xi^2) \;=\; \sigma^2 + \frac{w^2}{12}
\end{aligned}$$

From this we obtain

$$\sigma^2_{\rm PR}(0) := \sigma^2_{\rm PR} - C_d^2 z = \sigma^2_{\rm PRF} + \frac{w^2}{12}$$

By plotting $\sigma^2_{\rm PR}$ as a function of z, we can hence extract Cd from the slope and $\sigma^2_{\rm PRF}$ from the intercept with the finite pad pitch correction of $w^2/12$.

Cd Measurement

TU-TPC test at KEK cryo hall (Dec. 2007)

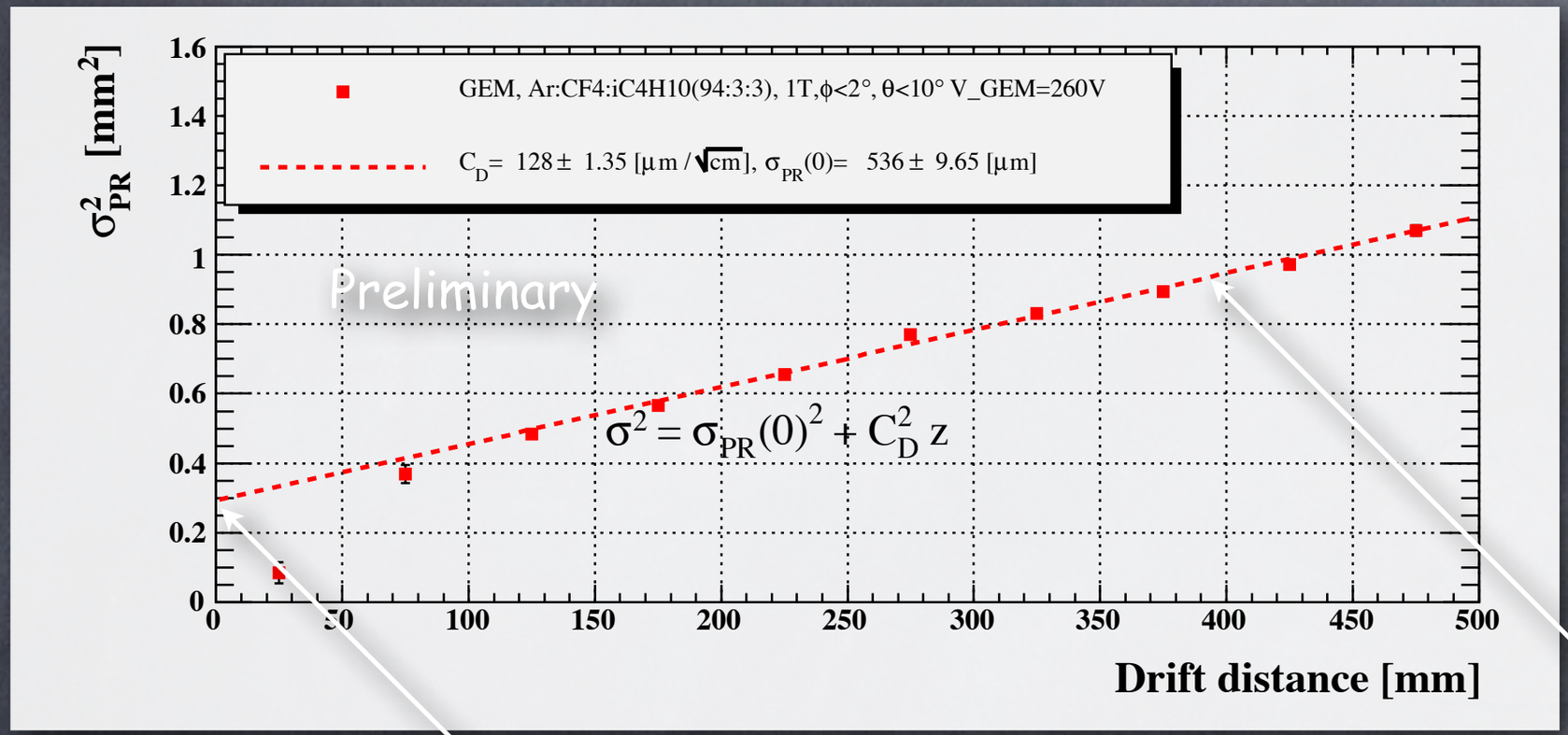

Assuming

$$v_{drift} = 4.2\,[\mathrm{cm}/\mu\mathrm{s}]$$

from drift time data, plot the apparent pad response function as a function of the drift distance. Then perform a straight-line fit.

From the intercept

$$\sigma^2_{\mathrm{PR}}(0) := \sigma^2_{\mathrm{PR}} - C_d^2 z = \sigma^2_{\mathrm{PRF}} + \frac{w^2}{12}$$

$$\begin{aligned} \sigma^2_{PRF} &= \sigma_{PR}(0)^2 - \frac{w^2}{12} \\ &= (270\,[\mu\mathrm{m}])^2 \end{aligned}$$

From the slope

$$C_D = 128\,[\mu\mathrm{m}/\sqrt{\mathrm{cm}}]$$

roughly consistent with what we expect from the diffusion in transfer and induction gaps.

Angular Pad Effect

Resolution degradation for inclined tracks

Consider an inclined track having an angle phi to the yz plane and an angle theta to the xy plane (pad plane). The projection of the track electrons to the xz plane is no longer point-like even if the cluster size is negligible for secondary ionizations. This extra charge spread adds up to that caused by diffusion. Consequently, the statistical fluctuation of the locations of the primary ionizations as well as that of the 2ndary ionizations cause additional contributions to the coordinate measurement error. The effect is further amplified by the gas gain fluctuations. The degradation of spatial resolution due to the finite phi is known as the angular pad effect and is inevitable as long as we use ordinary readout pads, since they break the rotational symmetry in the phi direction (notice that the symmetry breaking must be much softer in the case of pixel readout). If the theta is nonzero, the drift distance depends on where you are on the track and the average number of ionization electrons will be larger due to the longer track segment per pad row. As long as we use a short enough pad, the drift distance can be regarded as approximately constant within a pad row. We can hence assume that the effect of the finite theta can be taken into account by scaling Neff by the amount expected from the increase of the track segment length. For this reason we assume in what follows that the theta is zero unless otherwise stated.

Resolution Formula

Since TPC operates on the nice and old "gas physics"; ionization, diffusion, gas amplification and fluctuation, etc., it is possible for the GEM TPC (option (1)) to formulate a fully analytic expression of its spatial resolution to understand the LP TPC results, to optimize parameters of the GEM TPC, and to extrapolate them to the ILD TPC (JINST 9 C03002 (2014))

$$\sigma_x^2(z; w, L\tan\phi, C_d, N_{eff}, \hat{N}_{eff}, [f]) = [A] + \frac{1}{N_{eff}}[B] + [C] + \frac{1}{\hat{N}_{eff}}[D]$$

[A]: Hodoscope effect/S-shape at the short drift distances

$$[A] := \int_{-1/2}^{+1/2} d\left(\frac{\tilde{x}}{w}\right)\left(\sum_a (aw)\,\langle\langle F_a(\tilde{x} + y\tan\phi + \Delta x)\rangle_{\Delta x}\rangle_y - \tilde{x}\right)^2$$

diffusion-averaged & cluster position average charge centroid

systematics

asymptotic formula ([B] term)

$$\sigma_x^2 = \frac{1}{N_{eff}}(\sigma_0'^2 + C_d^2 z)$$

The constant term also scales as $1/N_{eff}$!

[B]: Diffusion + finite pad size term

$$[B] := \int_{-1/2}^{+1/2} d\left(\frac{\tilde{x}}{w}\right)\left\langle\left(\sum_a (aw)F_a(\tilde{x} + \Delta x) - \sum_a (aw)\,\langle F_a(\tilde{x} + \Delta x)\rangle_{\Delta x}\right)^2\right\rangle_{\Delta x}$$

$$\approx [A]_{z=0} + \sigma_d^2$$

diffusion-averaged charge centroid

displacement due to diffusion for a single electron

$$N_{eff} := \left[\left\langle\sum_{i=1}^{N} k_i \left\langle\left(\frac{G_{ij}}{\sum_{i=1}^{N}\sum_{j=1}^{k_i} G_{ij}}\right)^2\right\rangle_G^{\sum_{i=1}^{N} k_i}\right\rangle_{N,k}\right]^{-1}$$

: effective # electrons

[C]: Electronics noise

$$[C] := \left(\frac{\sigma_G}{\bar{G}}\right)^2 \left\langle\frac{1}{N^2}\right\rangle_N \sum_a (aw)^2$$

[D]: Angular pad effect

$$[D] := \frac{L^2\tan^2\phi}{12}$$

$$\hat{N}_{eff} \simeq \left[\left\langle\sum_{i=1}^{N}\left\langle\left(\frac{\sum_{j=1}^{k_i} G_{ij}}{\sum_{i=1}^{N}\sum_{j=1}^{k_i} G_{ij}}\right)^2\right\rangle_G^{k_i,\,\sum_{i=1}^{N} k_i}\right\rangle_{N,k}\right]^{-1}$$

: effective # clusters

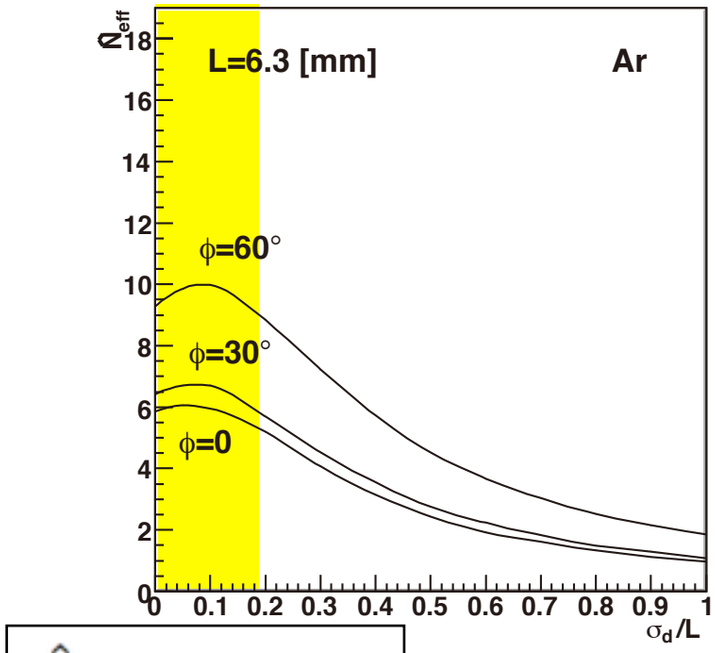

$$\hat{N}_{eff} \ll N_{eff}$$

$\sigma_{r\phi}$ quickly deteriorates with ϕ!

Comparison with Exp.

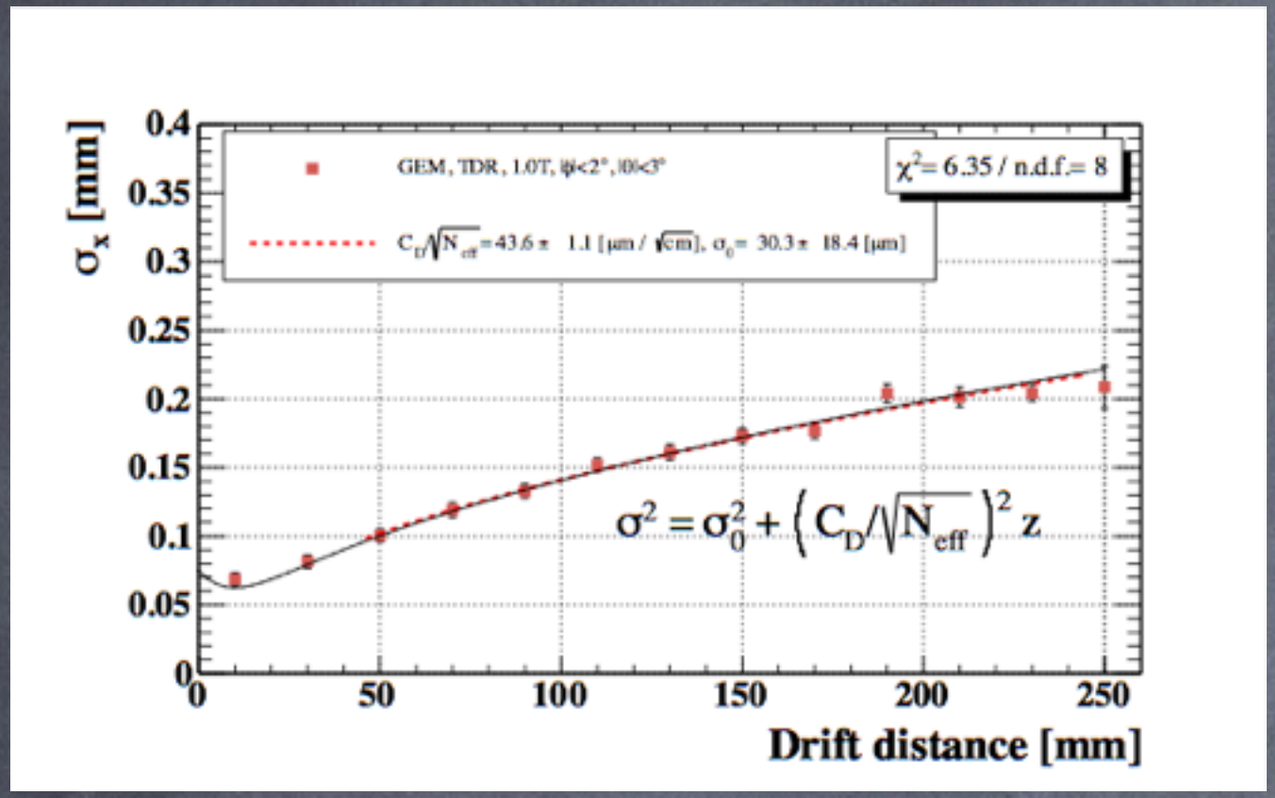

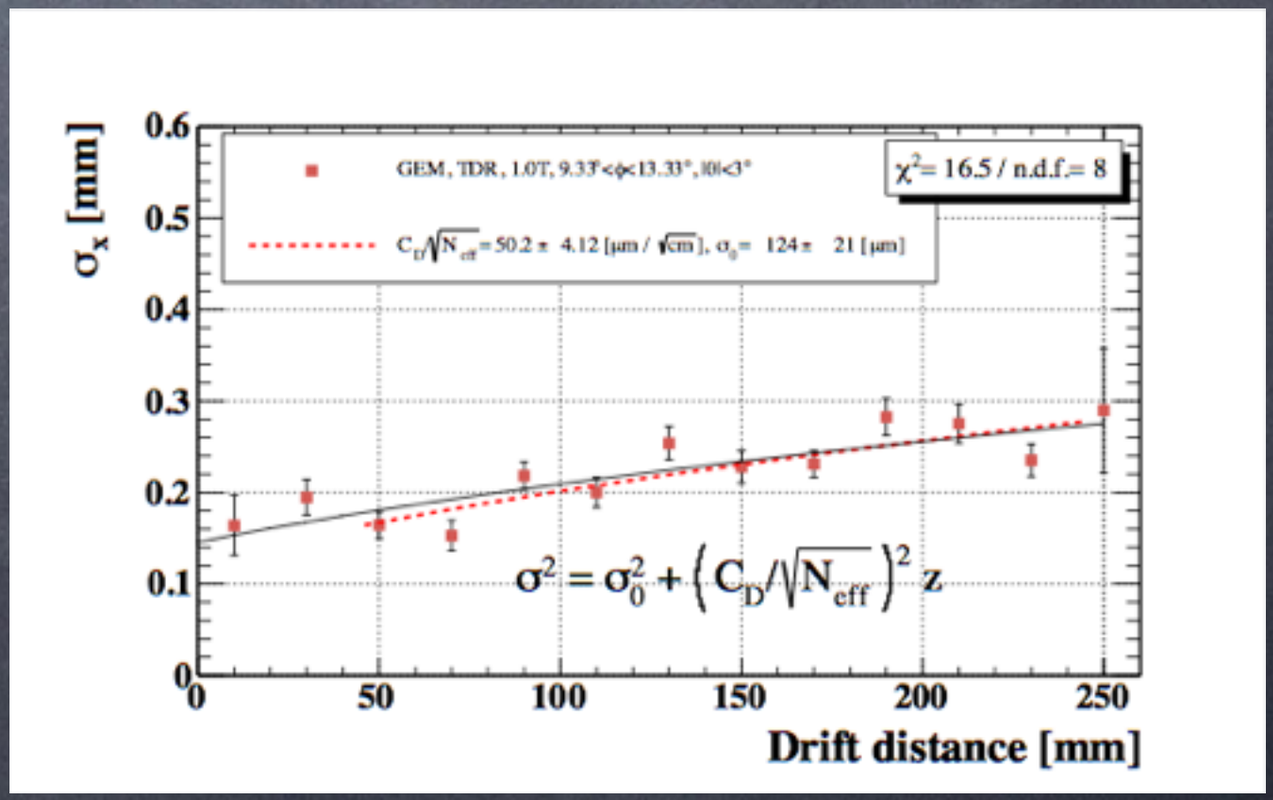

Ion Gate

Tracking Codes for LP TPC and ILD TPC

Tracking Code (MarlinTrk): now fully C++

$e^+e^- \rightarrow$ t tbar @1TeV

KEK developed Kalman Filter Package (KalTest)

Reconstructed Tracks

- The continuous tracking in TPC is very robust against the backgrounds (including the micro curlers) at ILC reaching 100% tracking efficiency (> 1GeV/c) except the forward region
- A Kalman filter based tracking code for TPC at ILC has been developed (Li Bo/ KF), and implemented in the MarlinTPC code for the beam test data analysis as well as to the new MarlinReco for the ILD physics simulation

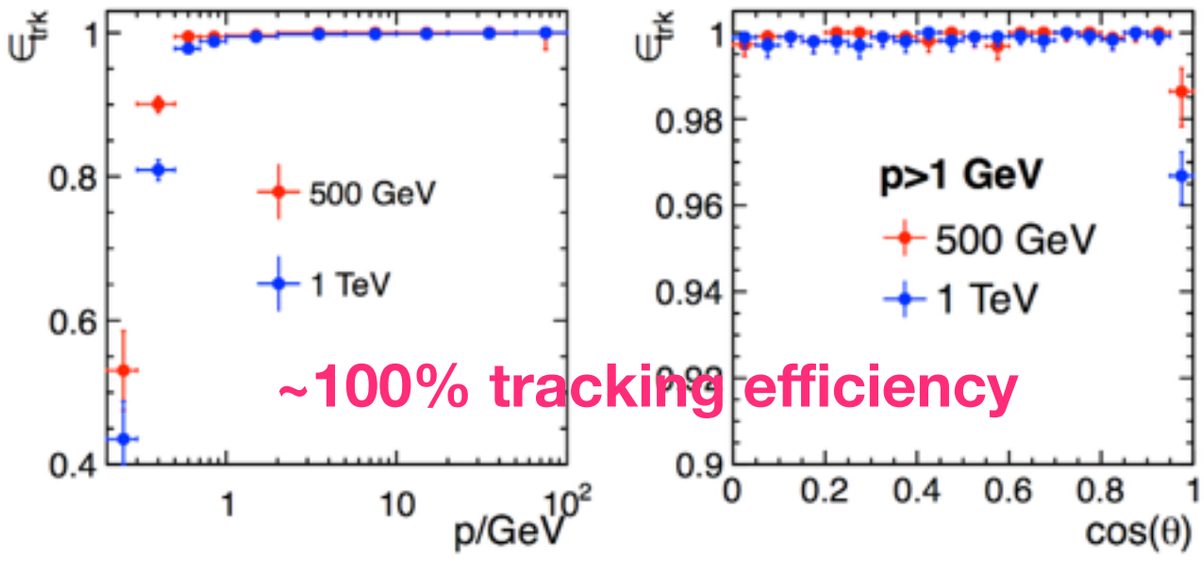

~100% tracking efficiency

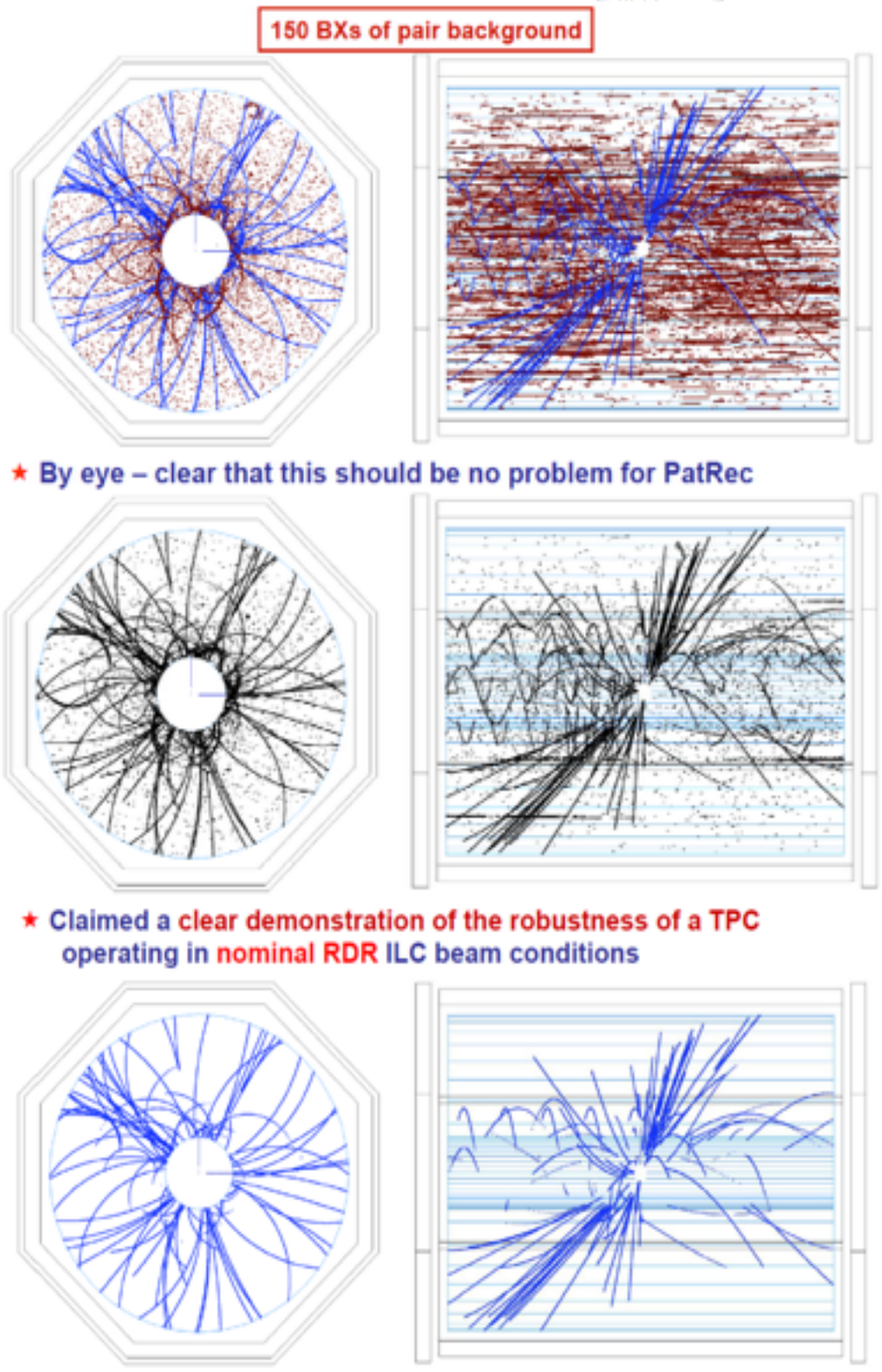

Despite the more realism (cracks, support structures, and service materials) brought in to the simulator,

PFA performance is now better than that of LoI!

Effects of Positive Ions and Ion Gating at ILC

Solve the Poisson equation for a given ion density distribution with proper boundary conditions. Then, estimate the distortion of drift electron trajectory by the Langevin equation (D. Arai and KF)

	without Gating Device	with Gating Device
Primary Ion	8.5 μm	8.5 μm
Secondary Ion	60 μm	0.01 μm
sum	70 μm	8.5 μm

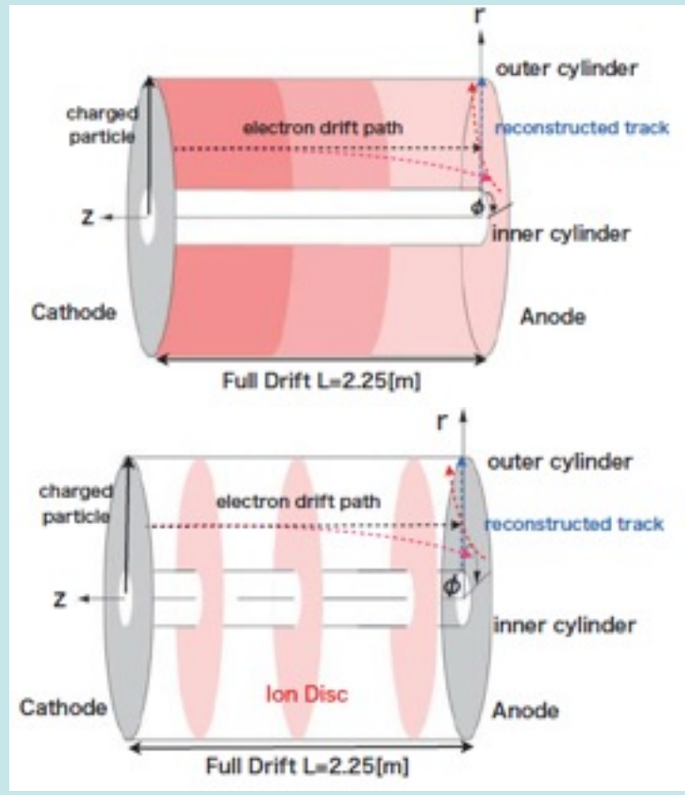

For the secondary ions from the amplification, we need an ion gate device for the ion feed back ratio of >10^{-3} (measured both for the triple GEM and Micromegas) at the gas gain of 1,000.

The current options of the ion gate are limited:

- **The traditional wire gate is expected to work, but introduces mechanical complications to the MPGD modules. We also need to check ExB effect.**
- **Thin GEM gate offers the electron transmission of only 50%@ 1T → 30% loss in the point resolution (Japanese LC TPC group).**
- **Try a larger geometric aperture with new fabrication method?**

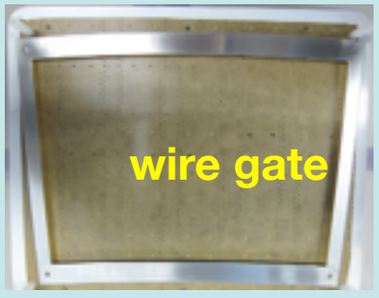

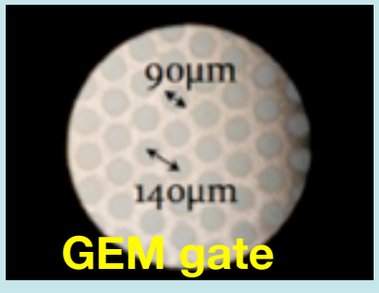

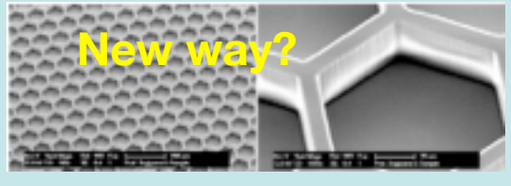

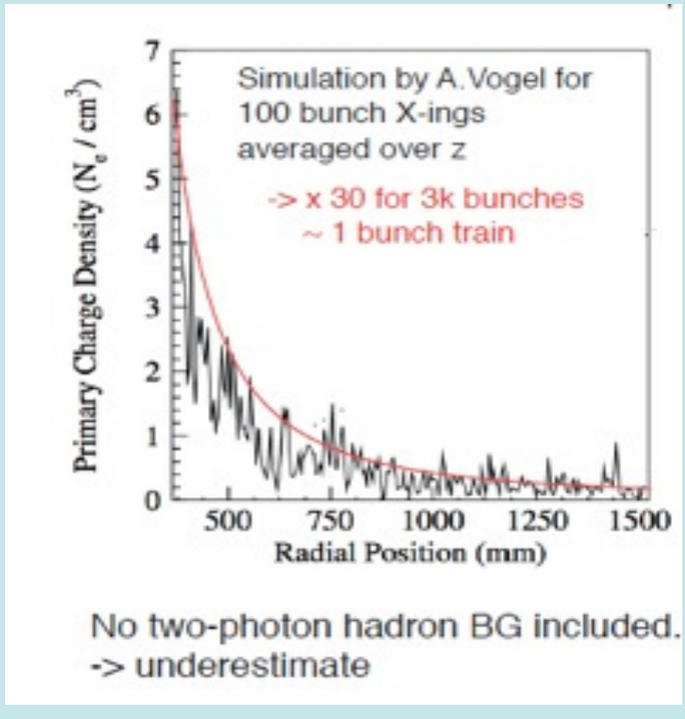

Poisson's equation

The E field in a region (D) is the sum of the E field (E0) without space charge in the corresponding region defined by the field shaping strips and the two terminating plates and the field (Eion) calculated with space charge in the virtual grounded conducting boundary of D.

$$\triangle\phi_0(\boldsymbol{x}) = 0$$
$$\triangle\phi_{\rm ion}(\boldsymbol{x}) = -4\pi\,\rho_{\rm ion}(\boldsymbol{x}) \qquad \text{in } \boldsymbol{x} \in D$$

$$\phi(\boldsymbol{x}) = \phi_0(\boldsymbol{x}) + \phi_{\rm ion}(\boldsymbol{x})$$

$$\longrightarrow \quad \boldsymbol{E} = \boldsymbol{E}_0 + \boldsymbol{E}_{\rm ion} = \boldsymbol{E}_0 - \nabla\phi_{\rm ion}(\boldsymbol{x})$$

Boundary Conditions

$$\phi_0(\boldsymbol{x}) = V_i \qquad \boldsymbol{x} \in C_i$$

$$\phi_{\rm ion}(\boldsymbol{x}) = 0 \qquad \boldsymbol{x} \in \partial D$$

All we need is Green's function for

$$\triangle G(\boldsymbol{x}, \boldsymbol{x'}) = -4\pi\delta(\boldsymbol{x} - \boldsymbol{x'})$$

$$G(\boldsymbol{x}, \boldsymbol{x'}) = 0 \qquad \boldsymbol{x} \in \partial D$$

E-field distortion is then given by superposition:

$$\phi_{\rm ion}(\boldsymbol{x}) = \int_D d^3\boldsymbol{x}\, G(\boldsymbol{x}, \boldsymbol{x'})\, \rho_{\rm ion}(\boldsymbol{x'})$$

Superposition makes life easy!

Green's function

Since the boundaries are most naturally expressed in the cylindrical coordinates (rin=a, rout=b, z=0, Z=L), the corresponding Green function is most conveniently expanded in terms of modified Bessel function as follows:

$$G(r,\varphi,z;r',\varphi',z') = \sum_{n=1}^{\infty}\sum_{m=-\infty}^{\infty} g_{mn}(r,r')\frac{1}{2\pi}e^{im(\varphi-\varphi')}\frac{2}{L}\sin(\beta_n z)\sin(\beta_n z')$$

where

$$g_{mn}(r,r') = \frac{4\pi\left[K_m(\beta_n a)I_m(\beta r_<) - I_m(\beta_n a)K_m(\beta_n r_<)\right]\left[K_m(\beta_n b)I_m(\beta r_>) - I_m(\beta_n b)K_m(\beta_n r_>)\right]}{\beta_n r'\left[I_m(\beta_n a)K_m(\beta_n b) - I_m(\beta_n b)K_m(\beta_n a)\right]\left[K_m(\beta_n r')I'_m(\beta_n r') - K'_m(\beta_n r')I_m(\beta_n r')\right]}$$

$$\beta_n = n\pi/L$$

If the charge distribution is uniform in phi as under our assumption, the phi-integral is trivial and we get

$$\phi_{\text{ion}}(r,z) = \sum_{n=1}^{\infty}\frac{8\pi}{\beta_n}\int_a^b dr'\,\frac{\left[K_0(\beta_n a)I_0(\beta r_<) - I_0(\beta_n a)K_0(\beta_n r_<)\right]\left[K_0(\beta_n b)I_0(\beta r_>) - I_0(\beta_n b)K_0(\beta_n r_>)\right]}{\left[I_0(\beta_n a)K_0(\beta_n b) - I_0(\beta_n b)K_0(\beta_n a)\right]\left[K_0(\beta_n r')I'_0(\beta_n r') - K'_0(\beta_n r')I_0(\beta_n r')\right]}$$
$$\sin(\beta_n z)\int_0^L \frac{dz'}{L}\,\sin(\beta_n z')\rho_{\text{ion}}(r',z')$$

Derivatives of the modified Bessel functions can be rewritten in terms of those of different orders:

$$I'_0(x) = I_1(x) \quad \text{and} \quad K'_0(x) = -K_1(x)$$

If we can assume that the charge distribution can be factorized into the phi part and the z part as $\rho_{\rm ion}(r', z') = \bar{\rho}_r(r')\,\hat{\rho}_z(z')$ with $\int dz'\,\hat{\rho}_z(z') = L$

we can further simplify the calculation and get the following for Er:

$$
\begin{aligned}
E_r(r,z) = -8\pi \sum_{n=1}^{\infty} \frac{\sin(\beta_n z)}{I_0(\beta_n a)K_0(\beta_n b) - I_0(\beta_n b)K_0(\beta_n a)} \int_0^L \frac{dz'}{L}\, \sin(\beta_n z')\hat{\rho}_z(z') \\
\Bigg[[K_0(\beta_n b)I_1(\beta r) + I_0(\beta_n b)K_1(\beta_n r)] \int_a^r dr'\, \frac{K_0(\beta_n a)I_0(\beta r') - I_0(\beta_n a)K_0(\beta_n r')}{K_0(\beta_n r')I_1(\beta_n r') + K_1(\beta_n r')I_0(\beta_n r')}\, \bar{\rho}_r(r') \\
+ [K_0(\beta_n a)I_1(\beta r) + I_0(\beta_n a)K_1(\beta_n r)] \int_r^b dr'\, \frac{K_0(\beta_n b)I_0(\beta r') - I_0(\beta_n b)K_0(\beta_n r')}{K_0(\beta_n r')I_1(\beta_n r') + K_1(\beta_n r')I_0(\beta_n r')}\, \bar{\rho}_r(r') \Bigg]
\end{aligned}
$$

where

$\beta_n = n\pi/L$

In the practical calculations, we have to sum up the series up to high enough “n”, which is determined by the ratio of the shortest and the largest scales that specify the charge distribution and the geometry of the boundary of the region in question.

For a thin disk or in the MPGD-gate gap, summation up to 500 or more is necessary, which in turn requires quadruple precision calculations for the modified Bessel functions.

Principle (continued)

Assuming that E0 is parallel with the B field, it will not contribute to the ExB effect.
(c.f.) the Langevin Equation

$$\boldsymbol{\omega} := \frac{(-e)\boldsymbol{B}}{mc}$$

$$\omega\tau \simeq 10 \text{ for T2K gas at B=3.5T}$$

$$\langle \boldsymbol{v} \rangle = \left(\frac{\tau}{1+(\omega\tau)^2} \right) \left[1 + (\omega\tau)\hat{\boldsymbol{B}}\times + (\omega\tau)^2 \hat{\boldsymbol{B}}\,\hat{\boldsymbol{B}}\cdot \right] \frac{e}{m}\boldsymbol{E}$$

If we write down the distortion of the velocity due to the distortion of the E-field in the longitudinal and transverse directions, we get

$$\Delta\langle \boldsymbol{v} \rangle = \frac{e}{m} \left(\frac{\tau}{1+(\omega\tau)^2} \right) \left[(1+(\omega\tau)^2)\Delta\boldsymbol{E}_{\parallel} + \boldsymbol{E}_{\perp} - (\omega\tau)\boldsymbol{E}_{\perp}\times\hat{\boldsymbol{B}} \right]$$

Numerically integrating this over the drift time by noting $\delta l_i = \langle v_{\parallel} \rangle \delta t_i$, we get the following formula for the distortion:

$$\begin{aligned} \langle \Delta\boldsymbol{x} \rangle &= \sum_{i=1}^{n} \frac{\Delta\langle \boldsymbol{v} \rangle_i}{\langle v_{\parallel} \rangle_i} \delta l_i \\ &\simeq \sum_{i=1}^{n} \delta l_i \left[-\frac{\Delta\boldsymbol{E}_{\parallel i}}{E_{\text{nom}}} - \left(\frac{1}{1+(\omega\tau)^2} \right) \frac{\boldsymbol{E}_{\perp i}}{E_{\text{nom}}} + \left(\frac{\omega\tau}{1+(\omega\tau)^2} \right) \frac{\boldsymbol{E}_{\perp i}\times\hat{\boldsymbol{B}}}{E_{\text{nom}}} \right] \end{aligned}$$

Key point: distortion is linear w.r.t. E-field distortion, and hence also w.r.t. space charge for a drift from the same z to the anode: Superposition makes life easy!

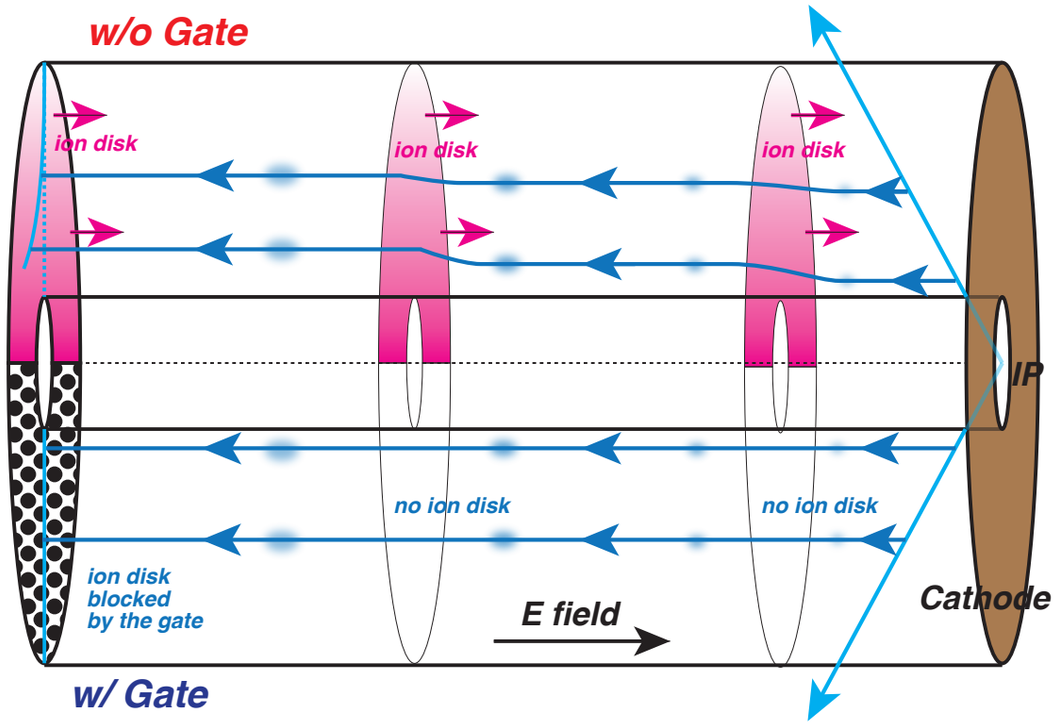
w/o Gate
ion disk
ion disk
ion disk
IP
no ion disk
no ion disk
ion disk
blocked
by the gate
E field
Cathode
w/ Gate

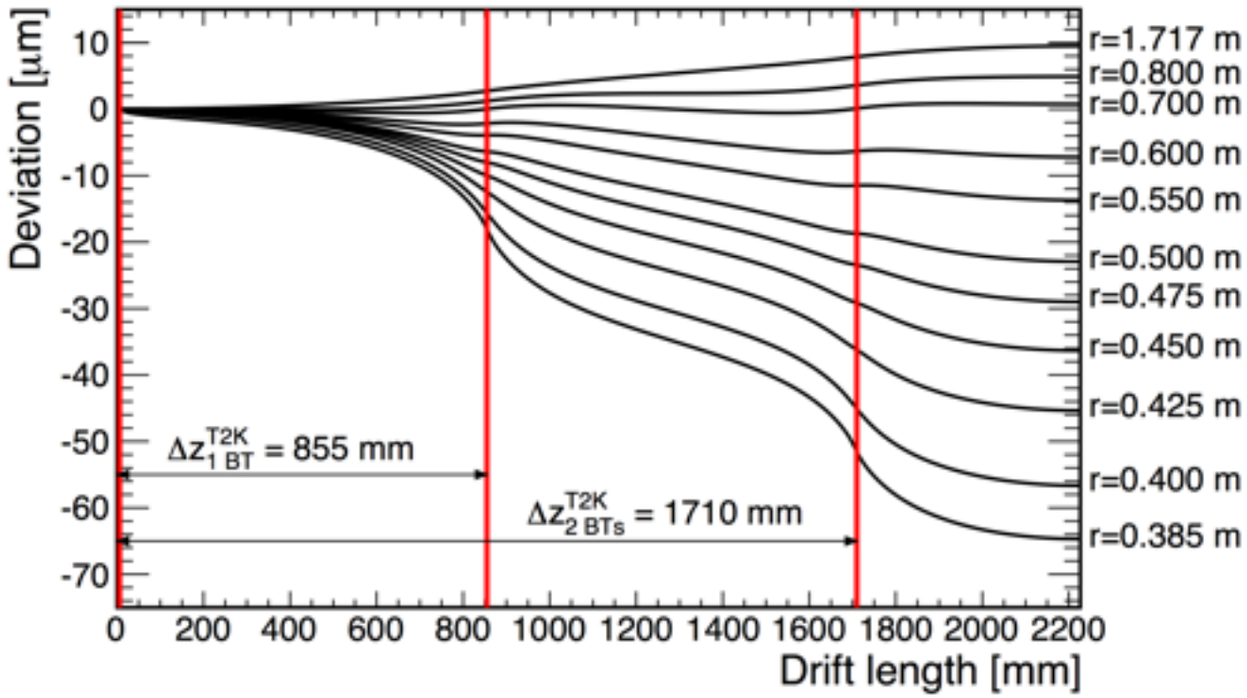
Deviation [μm]
10
0
-10
-20
-30
-40
-50
-60
-70
0
200
400
600
800
1000
1200
1400
1600
1800
2000
2200
Drift length [mm]
$\Delta z^{T2K}_{1\ BT}$ = 855 mm
$\Delta z^{T2K}_{2\ BTs}$ = 1710 mm
r=1.717 m
r=0.800 m
r=0.700 m
r=0.600 m
r=0.550 m
r=0.500 m
r=0.475 m
r=0.450 m
r=0.425 m
r=0.400 m
r=0.385 m